Quantum many-body dynamics of isolated systems close to and far away from equilibrium

Dissertation

(kumulativ)

Zur Erlangung des Grades eines
Doktors der Naturwissenschaften (Dr. rer. nat.)

dem Fachbereich Physik der Universität Osnabrück
vorgelegt von

Jonas Richter
aus Gifhorn

Osnabrück, Januar 2020

Contents

Publications

This cumulative dissertation is based on the publications [R1] - [R10].

[R1] Jonas Richter, Fengping Jin, Hans De Raedt, Kristel Michielsen, Jochen Gemmer, and Robin Steinigeweg,
"Real-time dynamics of typical and untypical states in nonintegrable systems",
Physical Review B **97**, 174430 (2018),

Preprint: https://arxiv.org/abs/1801.07031
Published version: https://doi.org/10.1103/PhysRevB.97.174430

[R2] Jonas Richter, Jacek Herbrych, and Robin Steinigeweg,
"Sudden removal of a static force in a disordered system: Induced dynamics, thermalization, and transport",
Physical Review B **98**, 134302 (2018),

Preprint: https://arxiv.org/abs/1808.00497
Published version: https://doi.org/10.1103/PhysRevB.98.134302

[R3] Jonas Richter and Robin Steinigeweg,
"Relation between far-from-equilibrium dynamics and equilibrium correlation functions for binary operators",
Physical Review E **99**, 012114 (2019),

Preprint: https://arxiv.org/abs/1711.00672
Published version: https://doi.org/10.1103/PhysRevE.99.012114

[R4] Jonas Richter and Robin Steinigeweg,
"Combining dynamical quantum typicality and numerical linked cluster expansions",
Physical Review B **99**, 094419 (2019),
© American Physical Society.
Preprint: `https://arxiv.org/abs/1901.02909`
Published version: `https://doi.org/10.1103/PhysRevB.99.094419`

[R5] Jonas Richter, Fengping Jin, Lars Knipschild, Jacek Herbrych, Hans De Raedt, Kristel Michielsen, Jochen Gemmer, and Robin Steinigeweg,
"Magnetization and energy dynamics in spin ladders: Evidence of diffusion in time, frequency, position, and momentum",
Physical Review B **99**, 144422 (2019),
© American Physical Society.
Preprint: `https://arxiv.org/abs/1811.02806`
Published version: `https://doi.org/10.1103/PhysRevB.99.144422`

[R6] Jonas Richter, Jochen Gemmer, and Robin Steinigeweg,
"Impact of eigenstate thermalization on the route to equilibrium",
Physical Review E **99**, 050104(R) (2019),
© American Physical Society.
Preprint: `https://arxiv.org/abs/1805.11625`
Published version: `https://doi.org/10.1103/PhysRevE.99.050104`

[R7] Ben N. Balz, Jonas Richter, Jochen Gemmer, Robin Steinigeweg,
and Peter Reimann,
"Dynamical typicality for initial states with a preset measurement statistics of several commuting observables",
in: Thermodynamics in the Quantum Regime: Fundamental Aspects and New Directions (Springer, Cham, 2019),
© Springer Nature.
Preprint: `https://arxiv.org/abs/1904.03105`
Published version: `https://doi.org/10.1007/978-3-319-99046-0_17`

[R8] Jonas Richter, Mats H. Lamann, Christian Bartsch, Robin Steinigeweg, and Jochen Gemmer,
"Relaxation of dynamically prepared out-of-equilibrium initial states within and beyond linear response theory",
Physical Review E **100**, 032124 (2019),
© American Physical Society.
Preprint: `https://arxiv.org/abs/1905.03292`
Published version: `https://doi.org/10.1103/PhysRevE.100.032124`

[R9] Jonas Richter, Niklas Casper, Wolfram Brenig, and Robin Steinigeweg,
"Magnetization dynamics in clean and disordered spin-1 XXZ chains",
Physical Review B **100**, 144423 (2019),
© American Physical Society.
Preprint: `https://arxiv.org/abs/1907.03004`
Published version: `https://doi.org/10.1103/PhysRevB.100.144423`

[R10] Jonas Richter, Fengping Jin, Lars Knipschild, Hans De Raedt, Kristel Michielsen, Jochen Gemmer, and Robin Steinigeweg,
"Exponential damping induced by random and realistic perturbations".
Preprint: `https://arxiv.org/abs/1906.09268`

In addition to the works [R1] - [R10], the following publication appeared during the final phase of the PhD, but will not be discussed in detail in this dissertation.

[R11] Jonas Richter, Dennis Schubert, and Robin Steinigeweg,
"Decay of spin-spin correlations in disordered quantum and classical spin chains".
Physical Review Research **2**, 013130 (2020),
© American Physical Society.
Preprint: `https://arxiv.org/abs/1911.09917`
Published version: `https://doi.org/10.1103/PhysRevResearch.2.013130`

Scientific Outreach

Results of this dissertation have been presented at the following international conferences and workshops.

Talks

- *"Impact of eigenstate thermalization on the route to equilibrium",*
  International workshop "Out-off-equilibrium dynamics in many-body systems",
  24.09.2018 - 26.09.2018, Osnabrück, Germany.

- *"Dynamics of densities and currents in spin ladders",*
  March meeting of the American Physical Society,
  04.03.2019 - 08.03.2019, Boston, USA.

- *"Dynamics of densities and currents in spin ladders",*
  Spring meeting of the German Physical Society,
  31.03.2019 - 05.04.2019, Regensburg, Germany.

- *"Tackling quantum many-body dynamics by typicality, numerical linked cluster expansion, and projection operator techniques",*
  International workshop "Fundamental Aspects of Statistical Mechanics and the Emergence of Thermodynamics in Non-Equilibrium Systems",
  23.09.2019 - 26.09.2019, Delmenhorst, Germany.

Posters

- *"Towards real-time dynamics of typical and untypical states in non-integrable systems",*
  Winter school "Numerical Methods for Strongly Correlated Quantum Systems",
  19.02.2018 - 23.02.2018, Marburg, Germany.

- *"Towards real-time dynamics of typical and untypical states in non-integrable systems",*
  March meeting of the American Physical Society,
  05.03.2018 - 09.03.2018, Los Angeles, USA.

- *"Towards real-time dynamics of typical and untypical states in non-integrable systems",*
  International workshop "Trends in Quantum Magnetism",
  04.06.2018 - 08.06.2018, Bad Honnef, Germany.

- *"Impact of eigenstate thermalization on the route to equilibrium",*
  International workshop "Out-off-equilibrium dynamics in many-body systems",
  24.09.2018 - 26.09.2018, Osnabrück, Germany.

- *"Magnetization and energy dynamics in spin ladders: Evidence of diffusion in time, frequency, position, and momentum",*
  International workshop "Nonequilibrium physics across boundaries",
  20.01.2019 - 24.01.2019, Rehovot, Israel.

- *"Relaxation dynamics after the removal of a static force: Binary operators and impact of eigenstate thermalization",*
  March meeting of the American Physical Society,
  04.03.2019 - 08.03.2019, Boston, USA.

- *"Relaxation dynamics after the removal of a static force: Binary operators and impact of eigenstate thermalization",*
  Spring meeting of the German Physical Society,
  31.03.2019 - 05.04.2019, Regensburg, Germany.

- *"Combining dynamical quantum typicality and numerical linked cluster expansions",*
  International workshop "Korrelationstage 2019",
  15.09.2019 - 20.09.2019, Dresden, Germany.

Quantum many-body dynamics of isolated systems close to and far away from equilibrium

Jonas Richter

Department of Physics,
University of Osnabrück,
Barbarastraße 7,
D-49076 Osnabrück,
Germany

Based on the works [R1] - [R10], this thesis tackles various aspects of the dynamics of interacting quantum many-body systems. Particular emphasis is given to the understanding of transport and thermalization phenomena in isolated (quasi) one-dimensional quantum spin models. Employing a variety of methods, these phenomena are studied both, close to equilibrium where linear response theory (LRT) is valid, as well as in far-from-equilibrium situations where LRT is supposed to break down. The main results of this thesis can be summarized as follows. First, it is shown that conventional hydrodynamic transport, i.e., diffusion, occurs in a number of (integrable and nonintegrable) quantum models and can be detected by looking at different signatures in position and momentum space as well as in the time and the frequency domain. Furthermore, the out-of-equilibrium dynamics resulting from a realistic class of initial states is explored. These states are thermal states of the model in the presence of an additional static force, but become nonequilibrium states when this force is eventually removed. Remarkably, it is shown that in some cases, the full time-dependent relaxation process can become independent of whether the initial state is prepared close to or far away from equilibrium. In this context, a new connection between the eigenstate thermalization hypothesis and linear response theory is unveiled. Finally, this thesis also reports progress on the development and improvement of numerical and (semi-)analytical techniques to access the dynamics of quantum many-body systems. Specifically, a novel combination of dynamical quantum typicality and numerical linked cluster expansions is employed to study current-current correlation functions in chain and ladder geometries in the thermodynamic limit.

CONTENTS

I. INTRODUCTION

Nonequilibrium processes involving the collective behavior of many degrees of freedom are omnipresent in our everyday life. Examples include the mixing of cold milk with hot coffee or, slightly more sophisticated, the diffusion of oxygen from our blood into the cells. Moreover, we know from experience that such processes (in the absence of some force maintaining the out-of-equilibrium conditions) evolve towards a stationary equilibrium state at long times. This process is called *thermalization* [12, 13].

Given a many-body system in thermal equilibrium, *statistical mechanics* provides an exceptionally successful framework to describe its macroscopic properties [14]. For instance, consider a gas which is initially confined to the right half of a box. At some point in time, the barrier separating the two halves of the box is removed. After waiting for a sufficiently long time, we then expect that the gas has thermalized, i.e., that it homogeneously fills the entire volume. Remarkably, for this new equilibrium state, statistical mechanics allows to make accurate predictions for macroscopic quantities, e.g., the pressure, without requiring precise knowledge about the positions or velocities of the individual gas particles. Far away from equilibrium, on the contrary, such a universal concept is absent. Instead, describing the state of the gas in an out-of-equilibrium situation usually requires to track the dynamics of each particle with respect to the underlying microscopic equations of motion.

While thermalization is a common observation, the opposite process is hardly ever encountered, i.e., after filling the whole volume, it seems inconceivable that all gas particles spontaneously move back to one half of the box. Speaking differently, thermalization is an *irreversible* process. This apparent ir-

reversibility is formulated in the second law of thermodynamics as the fact that the entropy of a system can never decrease. In contrast, however, the laws which govern the microscopic dynamics are *symmetric* in time. In view of this fact, it seems almost paradoxical why many-body systems reliably reach a thermal equilibrium state. Bridging this gap between the reversible microscopic equations of motion and the irreversible nature of thermalization has a long history (see e.g. [12, 13, 15, 16] and references therein). Ranging back to ideas of Boltzmann, a notable concept to explain thermalization in the case of classical mechanics is *ergodicity*, which asserts that the time spent by a classical trajectory in some volume of the phase space is proportional to the size of this volume. Moreover, it is now understood that the nonlinear equations of motion can cause the emergence of deterministic *classical chaos* and the onset of thermodynamic behavior [17]. However, since the microscopic laws of nature fundamentally obey quantum mechanics, developing an understanding for the occurrence of thermalization in *quantum systems* is vitally important. In fact, investigating the out-of-equilibrium dynamics in quantum many-body systems and studying their dynamical relaxation towards equilibrium is a central topic of this dissertation, with particular focus on the dynamics of so-called *isolated* systems.

Given an isolated quantum system, the time evolution of a pure state $|\psi(t)\rangle$ is unitary and generated by the Schrödinger equation,

$$i\partial_t |\psi(t)\rangle = \mathcal{H} |\psi(t)\rangle \ , \tag{1}$$

where i is the imaginary unit, $\mathcal{H}$ denotes the system's Hamiltonian, and the reduced Planck constant $\hbar$ has been set to unity. At first, one might be tempted to ask why one should be concerned with such systems at all, since, in the very end, no system can be perfectly isolated from the influence of an environment. Not surprisingly, the study of *open* quantum systems is an active area of research in its own right [18]. Nevertheless, quantum many-body systems in strict isolation have attracted continuously increasing attention in recent years [19, 20]. This upsurge of interest is not least due to major experimental advancements. New experimental platforms such as cold atoms in optical lattices as well as systems of trapped ions offer a high amount of control over many degrees of freedom, and open the possibility to explore the dynamics of tailored Hamiltonians and initial states [21, 22]. Importantly, these systems can be very well isolated from their environment such that the time evolution, at least on short to intermediate time scales, is unitary and given by Eq. (1). Motivated by these experimental achievements, there has been rejuvenated interest also from the theoretical side to reconsider the (aforementioned) long-standing questions on thermalization in isolated quantum systems [12, 13, 17, 19, 20], which have been addressed already in the early works by von Neumann [23]. In the last decades, substantial progress in this context has been made thanks to the development of fresh theoretical concepts such as the *typicality* of pure quantum states [24, 25, 26, 27, 28] (see also Sec. II.D and [R7]), and the *eigenstate thermalization hypothesis* (ETH) [29, 30, 31], which provides a microscopic explanation of thermalization on the basis of individual eigenstates (see Sec. II.C).

Generally, theoretical studies of interacting quantum systems are challenging. While analytical solutions are comparatively rare, numerical simulations of quantum many-body dynamics are tremendously difficult as well. This is not least caused by the fact that the dimension of the Hilbert space grows exponentially in the number of degrees of freedom. Nevertheless, the ever-increasing amount of computational resources and the availability of large-scale supercomputers have been ideally complemented by the development of sophisticated numerical methods [32], which, in combination, has lead to enormous progress (see also Sec. II.D). Most of the results presented in this thesis have been obtained from the implementation and application of state-of-the-art numerical methods. Moreover, this thesis also contributes to the development and improvement of numerical and (semi-)analytical techniques to tackle the dynamics of quantum many-body systems (see Sec. III.C).

Given an isolated quantum system with time-independent Hamiltonian, the only possibility to induce a nonequilibrium situation is the preparation of suitable out-of-equilibrium initial states. To this end, a common preparation scheme is a so-called quantum quench [33]. In such a quench protocol, the system is typically prepared in an eigenstate $|\psi_0\rangle$ of an initial Hamiltonian $\mathcal{H}_i$. At some point in time, say at $t = 0$, some parameter (e.g. the interaction strength) of $\mathcal{H}_i$ is suddenly varied such that $|\psi_0\rangle$ is a nonequilibrium state and evolves in time with respect to the final Hamiltonian $\mathcal{H}_f$. Studying the out-of-equilibrium dynamics resulting from sudden quench protocols is one line of research in this thesis. In particular, while the ETH explains the mere existence of thermalization, much less is known on the full time-dependent relaxation process prior to equilibration [34]. In this thesis, we shed light on this route to equilibrium by considering a realistic class of initial states which can be prepared close to as well as far away from equilibrium. Here, a controlled point of reference is provided by the theory of linear response, which is known to describe the dynamics in situations close to equilibrium.

Linear response theory (LRT) constitutes a major cornerstone of nonequilibrium statistical mechanics [35]. As its name suggests, LRT states that for a weakly perturbed system, the main contribution of the system's response is linear in the perturbation. Moreover, the response of the system in this case can be remarkably expressed in terms of time-dependent *cor-*

relation functions evaluated exactly at equilibrium. In this thesis, LRT plays an important role. On the one hand, for the quantum quench protocols mentioned above, we scrutinize the validity range of linear response theory in far-from-equilibrium situations and analyze its interplay with the eigenstate thermalization hypothesis. On the other hand, LRT also provides a convenient framework to study transport properties of quantum many-body systems, i.e., the dynamics and relaxation of local densities whose sum over the whole system is a conserved quantity. In this context, it is an intriguing question if and how conventional hydrodynamic transport, i.e., diffusion, can arise in isolated quantum systems undergoing unitary time evolution [36].

Preliminary remarks and scope of this thesis

This cumulative dissertation is based on the publications [R1] - [R10]. While the dynamics of quantum many-body systems is a vast field of research, the present text does not attempt to provide an exhaustive overview. Instead, it should be understood as a supporting document which helps to access the content of the publications. Moreover, while citations are kept to a minimum (≈ 100) throughout this text, a more detailed list of references can be found in the original publications [R1] - [R10].

This work is structured as follows. In Sec. II, an overview is given of the theoretical background which is used throughout Refs. [R1] - [R10]. Specifically, low-dimensional quantum spin systems are introduced in Sec. II.A as convenient models to investigate transport and thermalization phenomena in quantum many-body systems. Section II.B then discusses time-dependent equilibrium correlation functions and their connection to transport coefficients within the theory of linear response. Moreover, Sec. II.C considers the nonequilibrium dynamics of isolated quantum systems and explains how the emergence of thermodynamic behavior in such systems can be understood from the eigenstate thermalization hypothesis. Eventually, in Sec. II.D, different numerical methods to study the dynamical properties of quantum many-body systems are presented, where particular emphasis is given to dynamical quantum typicality and numerical linked cluster expansions.

The main results of this dissertation can be found in Sec. III, which provides a guide to the publications [R1] - [R10]. In particular, the papers have been grouped into the three categories (i) *Transport and the emergence of diffusion in quantum models*, (ii) *Nonequilibrium dynamics close to and far away from equilibrium*, and (iii) *Development of numerical and (semi-)analytical approaches*. While this classification is certainly not unique and some papers may well fit into multiple categories, the intention of this sorting is to clarify the relationships of the papers among each other. Finally, in Sec. IV, the results of this thesis are summarized and an outlook on open questions and future directions of research is given.

II. THEORETICAL BACKGROUND

A. Low-dimensional quantum spin models

Lattice models of interacting spins arguably represent one of the simplest classes of quantum many-body systems. In these models, quantum spins are defined on discrete lattice sites and interact, for instance, via a Heisenberg exchange [37],

$$\mathcal{H} = \sum_{l,l'} J_{ll'} \mathbf{S}_l \cdot \mathbf{S}_{l'} \ , \tag{2}$$

where the couplings $J_{ll'}$ between two sites l and l' can be either ferromagnetic ($J_{ll'} < 0$) or antiferromagnetic ($J_{ll'} > 0$). Moreover, the $\mathbf{S}_l = (S_l^x, S_l^y, S_l^z)$ denote three-component quantum spin-S operators fulfilling the commutator algebra $[S_l^x, S_{l'}^y] = i S_l^z \delta_{ll'}$ with cyclic extensions. While the Hamiltonian (2) can in principle be studied for arbitrary lattice geometries and couplings, the present thesis is especially concerned with (quasi) one-dimensional chain or ladder systems. Specifically, a central model in this thesis is the one-dimensional and anisotropic Heisenberg model, also known as the XXZ chain,

$$\mathcal{H}_{\mathrm{XXZ}} = J \sum_{l=1}^{L} \left(S_l^x S_{l+1}^x + S_l^y S_{l+1}^y + \Delta S_l^z S_{l+1}^z \right) \ , \tag{3}$$

where L is the number of lattice sites, Δ is an anisotropy in the z direction, and $J > 0$ from now on denotes the antiferromagnetic coupling constant, which here acts only between nearest neighbors. Note that we often consider systems with periodic boundary conditions where $S_{L+1}^{x,y,z} = S_1^{x,y,z}$.

With the exception of Ref. [R9], this thesis focuses on models consisting of spin-1/2 degrees of freedom (i.e. qubits). In this case, the local Hilbert space of a single spin is spanned by the two basis vectors $|\uparrow\rangle$ and $|\downarrow\rangle$. Moreover, the spin operators $S_l^{x,y,z}$ are defined in terms of the Pauli matrices,

$$\sigma^x = \begin{pmatrix} 0 & 1 \\ 1 & 0 \end{pmatrix}, \ \sigma^y = \begin{pmatrix} 0 & -i \\ i & 0 \end{pmatrix}, \ \sigma^z = \begin{pmatrix} 1 & 0 \\ 0 & -1 \end{pmatrix} \ , \tag{4}$$

where the operator $S_l^{x,y,z}$ in the full many-body Hilbert space with dimension $d = 2^L$ has to be understood as ($\hbar = 1$ again)

$$S_l^{x,y,z} = \underbrace{\mathbb{1}_2 \otimes \mathbb{1}_2 \otimes \cdots}_{l-1} \otimes \tfrac{1}{2}\sigma^{x,y,z} \otimes \underbrace{\mathbb{1}_2 \otimes \cdots \otimes \mathbb{1}_2}_{L-l} \ . \tag{5}$$

Eventually, the Jordan-Wigner transformation provides an instructive mapping between spin-1/2 oper-

ators and spinless fermions according to [38],

$$S_l^+ = c_l^\dagger e^{i\pi \sum_{j<l} n_j} \ , \tag{6}$$

$$S_l^- = c_l e^{-i\pi \sum_{j<l} n_j} \ , \tag{7}$$

$$S_l^z = n_l - \tfrac{1}{2} \ , \tag{8}$$

where we have introduced the raising and lowering operators $S_l^\pm = S_l^x \pm i S_l^y$. Moreover, $c_l^\dagger$ (c_l) creates (annihilates) a fermion at lattice site l, and $n_l = c_l^\dagger c_l$ is the fermionic occupation number operator. The identification of spin-1/2 operators with spinless fermions is rather plausible due to their identical local Hilbert-space dimensions. As becomes evident from Eq. (8), a spin-up state $|\uparrow\rangle$ is associated with an occupied lattice site, while a spin-down state $|\downarrow\rangle$ corresponds to an empty site. (Due to the Pauli principle, there can only be one fermion per site.) Note that the phase $\exp(\pm i\pi \sum_{j<l} n_j)$ in Eqs. (6) and (7) counts the number of occupied sites on the left of site l, and guarantees that the fermions fulfill their appropriate anti-commutation algebra, $\{c_l^\dagger, c_{l'}\} = \delta_{ll'}$, whereas spins on different lattice sites commute. Using the Jordan-Wigner transformation (6) - (8), it is straightforward to show that Eq. (3) can be written as [39]

$$\mathcal{H}_{\mathrm{JW}} = J \sum_{l=1}^{L} \Bigg[\frac{1}{2} \left(c_l^\dagger c_{l+1} + c_{l+1}^\dagger c_l \right) + \Delta \left(n_l - \frac{1}{2} \right) \left(n_{l+1} - \frac{1}{2} \right) \Bigg] \ . \tag{9}$$

Remarkably, for the one-dimensional model with nearest-neighbor couplings, the Jordan-Wigner phases cancel out, and the spin-1/2 XXZ chain translates into a tight-binding model of interacting spinless fermions. In this representation, it also becomes obvious that the xx and yy terms in Eq. (3) correspond to the kinetic part of the Hamiltonian (i.e. the hopping of fermions), while the zz terms represent the actual interaction.

Eventually, let us note that low-dimensional spin systems are not just toy models. In fact, spin chains such as Eq. (3) are relevant to describe the properties of various Mott insulators, where (quasi) one-dimensional structures are realized within the bulk materials [40]. Moreover, despite their apparent simplicity, those models can possess rich phase diagrams and feature exotic physical phenomena [41]. In this dissertation, low-dimensional spin models serve as prototypical examples of interacting quantum many-body systems and are used to study fundamental questions on the emergence of statistical mechanics in isolated quantum systems.

Integrable and nonintegrable models

An important concept is the distinction between integrable and nonintegrable models. In the case of classical mechanics, a Hamiltonian system with N degrees of freedom is integrable if it has N independent conservation laws which are mutually commuting under the Poisson bracket [42]. Due to these conserved quantities, the dynamics in such models is strongly constrained and fails to explore the full phase space, i.e., integrable models are nonergodic. On the contrary, if there are less conservation laws than degrees of freedom, then a classical model is nonintegrable and trajectories can become chaotic.

It might be fair to say that there is less agreement on the notion of integrability in the quantum realm [43]. First of all, given a Hilbert space of dimension d and some Hamiltonian $\mathcal{H}$, there always exist d mutually commuting operators that also commute with $\mathcal{H}$, namely, the projections $|n\rangle\langle n|$ on the individual eigenstates of $\mathcal{H}$. Nevertheless, not every quantum system is called integrable.

From a practical point of view, quantum-integrability often refers to the fact that the model can, in some sense, be solved exactly. As a simple example, consider the Hamiltonian (3) with $\Delta = 0$, i.e., the XX chain. In the Jordan-Wigner language, this spin chain corresponds to a one-dimensional model of free fermions which, by means of a Fourier transform, $c_q = \sqrt{1/L} \sum_{l=1}^{L} e^{iql} c_l$, can be easily diagonalized,

$$\mathcal{H}_{XX} = \sum_q E_q c_q^\dagger c_q \ , \tag{10}$$

where the eigenenergies are given by $E_q = J\cos(q)$, and the sum runs over the full set of discrete lattice momenta q.

Not only free models can be solved exactly (in a similar sense). In fact, the XXZ chain (3) remains integrable also for $\Delta \neq 0$ in terms of the so-called Bethe ansatz [44]. Furthermore, for quantum-integrable models such as the XXZ chain, it is possible to construct an extensive set of (quasi) local conservation laws [45], which is reminiscent of the definition of integrability in the classical case. (Note that the crucial aspect here is locality, whereas the aforementioned projections $|n\rangle\langle n|$ are highly nonlocal objects.)

Eventually, another characteristic which is commonly used to distinguish between integrable and nonintegrable quantum models is the energy-level statistics, i.e., the distribution of gaps between adjacent energy eigenvalues E_n and E_{n+1}. Conceptually, this idea dates back to works by Wigner and Dyson who found that the eigenvalues of complicated Hamiltonians can be understood from the spectrum of random matrices [46]. Specifically, given a real and symmetric matrix with entries drawn from a Gaussian distribution (the so-called Gaussian orthogonal ensemble), the distribution $P(s)$ of level spacings approximately follows,

$$P(s) \propto s \exp(-\alpha s^2) \ , \tag{11}$$

where $\alpha > 0$ is a constant coefficient, and Eq. (11) is

known as Wigner-Dyson distribution [13]. Later on, it has been conjectured that the energy levels of quantum systems with nonintegrable (i.e. chaotic) classical counterpart are described by Eq. (11) [47], whereas the level statistics of quantum models with integrable classical counterpart follow a Poissonian distribution, $P(s) \propto e^{-s}$ [48]. An important difference between these two distributions is the fact that eigenvalues of chaotic models repel each other, i.e., $P(s \to 0) \to 0$, while level repulsion is absent in the case of integrable models. Furthermore, it has been found numerically that the above conjectures also apply to quantum many-body systems where no classical counterpart exists (such as, e.g., the low-dimensional spin models considered in this thesis). For instance, starting from the integrable XXZ chain (3), $P(s)$ is found to change from a Poissonian to a Wigner-Dyson distribution upon adding an integrability-breaking perturbation [49] (see also Fig. 2 of Ref. [R1]). As a consequence, nonintegrable quantum models (even without classical limit) are often called chaotic or ergodic [13].

In this thesis, it is a recurrent theme to contrast integrable and nonintegrable models with respect to their transport and thermalization properties. In this context, the Hamiltonians (3) or (9) represent convenient starting points for our analysis, and will often be complemented by additional integrability-breaking terms (details on these modifications are given in Sec. III). Eventually, it is worth emphasizing that although the XXZ chain is integrable and solvable by the Bethe ansatz, this does by no means imply that all its dynamical properties are known exactly.

B. Transport coefficients and correlation functions

Given the XXZ chain (3), it is easy to convince oneself that the total magnetization S^z is a conserved quantity,

$$[S^z, \mathcal{H}_{\mathrm{XXZ}}] = 0 \ , \quad \text{with } S^z = \sum_{l=1}^{L} S_l^z \ . \tag{12}$$

In fact, all models considered in this thesis fulfill the property (12). In other words, given an inhomogeneous distribution of S_l^z, it is not possible that excess magnetization in some part of the system is simply annihilated, while missing magnetization in another part of the system is created. Instead, in order for the system to reach thermal equilibrium, the magnetization has to be transported through the whole system. Since such transport processes are comparatively slow, they are also relevant to the understanding of equilibration and thermalization time scales in quantum systems [50]. Moreover, apart from these fundamental issues, the proper theoretical understanding of transport phenomena in low-dimensional spin systems is also of importance in order to pave the way for potential spin-based technologies in the future [51].

There exist various approaches to analyze the transport properties of quantum systems. In this thesis, the framework of linear response theory is used, where transport coefficients are calculated from time-dependent correlation functions evaluated in an equilibrium ensemble [35]. For the sake of illustration, the following discussion focuses on the transport of magnetization, where the spin current results from a gradient of the magnetic field. (Generalizations to other conserved quantities are in principle possible.) A central result of LRT is the so-called Kubo formula, which connects the (real part of the) frequency-dependent conductivity to dynamical current-current correlation functions [35],

$$\mathrm{Re}\ \sigma(\omega) = \frac{1 - e^{-\beta\omega}}{\omega L} \mathrm{Re} \int_0^\infty e^{i\omega t} \langle j(t) j \rangle_{\mathrm{eq}} \ \mathrm{d}t \ , \tag{13}$$

where $\beta = 1/T$ is the inverse temperature and $j(t) = e^{i\mathcal{H}t} j e^{-i\mathcal{H}t}$ is the time-evolved spin-current operator in the Heisenberg picture. The brackets $\langle \bullet \rangle_{\mathrm{eq}}$ denote the (canonical) equilibrium expectation value,

$$\langle j(t) j \rangle_{\mathrm{eq}} = \frac{\mathrm{Tr}[j(t) j \ e^{-\beta\mathcal{H}}]}{\mathcal{Z}} \ , \tag{14}$$

where $\mathcal{Z} = \mathrm{Tr}[e^{-\beta\mathcal{H}}]$ is the partition function. Specifically, the total spin current $j = \sum_l j_l$ is given by the sum over local current densities j_l, which fulfill a lattice continuity equation [52],

$$\frac{\mathrm{d}}{\mathrm{d}t} S_l^z = i[\mathcal{H}, S_l^z] = j_{l-1} - j_l \ . \tag{15}$$

In the case of the XXZ chain (3), j takes on the form [52]

$$j = J \sum_{l=1}^{L} \left(S_l^x S_{l+1}^y - S_l^y S_{l+1}^x \right) \ , \tag{16}$$

which consists of a right-moving and a left-moving contribution, i.e., the total current vanishes in thermal equilibrium, $\langle j \rangle_{\mathrm{eq}} = 0$. Assuming that $\langle j(t) j \rangle_{\mathrm{eq}}$ is well-behaved such that the integral in Eq. (13) converges (more details on this issue are given below), an important quantity is the dc conductivity σ_{dc}, which follows in the zero-frequency limit of the real part of $\sigma(\omega)$,

$$\sigma_{\mathrm{dc}} = \lim_{\omega \to 0} \mathrm{Re}\ \sigma(\omega) \ . \tag{17}$$

Generally, dynamical processes (such as transport) depend on the time scales considered. In this context, a useful quantity is the time-dependent diffusion coefficient $D(t)$ at formally infinite temperature [53],

$$D(t) = \frac{1}{\chi} \int_0^t \frac{\mathrm{Re}\ \langle j(t') j \rangle_{\mathrm{eq}}}{L} \ \mathrm{d}t' \ , \tag{18}$$

where $\langle \bullet \rangle_{\mathrm{eq}}$ reduces to $\mathrm{Tr}[\bullet]/d$ at $\beta = 0$, and the infinite-temperature susceptibility $\chi = \mathrm{Tr}[(S^z)^2]/L -$

$\mathrm{Tr}[S^z]^2/L$ is equal to $\chi = 1/4$. The time dependence of $D(t)$ can be understood as follows. In the simplest case, the model under consideration is a perfect conductor such that an initially induced current does not decay, i.e., $\langle j(t)j\rangle_{\mathrm{eq}} = \mathrm{const.}$ (An example is provided further below.) Then, it is easy to see from Eq. (18) that $D(t) \propto t$ grows linearly in time. This ideal dissipationless transport behavior is called *ballistic*. More generically, however, one might expect that $\langle j(t)j\rangle_{\mathrm{eq}}$ is not conserved exactly, eventually starts to decay and (approximately) vanishes at long times. Also in this case, one finds that $D(t) \propto t$ grows linearly for sufficiently short times (where $\langle j(t)j\rangle_{\mathrm{eq}}$ has not significantly decayed yet). In other words, transport is ballistic below the mean-free time. For times above the mean-free time, however, the contributions to the integral (18) become smaller and smaller, such that $D(t)$ eventually saturates to a time-independent plateau. In this case, the long-time value $D(t \to \infty) = D$ becomes the *diffusion constant* which is related to σ_{dc} by an Einstein relation,

$$D = \frac{\sigma_{\mathrm{dc}}}{\chi} \ , \tag{19}$$

where the infinite-temperature dc conductivity should be understood as $\sigma_{\mathrm{dc}} = \lim_{\beta\to 0,\omega\to 0} \mathrm{Re}\,\sigma(\omega)/\beta$. However, there can also be cases where the dynamics of $\langle j(t)j\rangle_{\mathrm{eq}}$ is more complicated and transport is neither diffusive nor ballistic. Generally, the time-dependence of $D(t)$ might be written as $D(t) \propto t^\alpha$, where transport is called *superdiffusive* for $0 < \alpha < 1$ and *subdiffusive* for $\alpha < 0$.

To proceed, more detailed information about the transport properties can be obtained by studying the correlation functions of local densities [54],

$$C_{l,l'}(t) = \langle S^z_l(t) S^z_{l'}\rangle_{\mathrm{eq}} \ . \tag{20}$$

These spatio-temporal correlations can be understood as the spreading of a single spin excitation, which is created at lattice site l' and moves with respect to an equilibrium many-body background at a given temperature. Furthermore, it is instructive to consider the respective density modes $C_q(t)$ in momentum space (sometimes referred to as the intermediate structure factor [54]), which are related to the real-space correlations $C_{l,l'}(t)$ by means of a lattice Fourier transform,

$$C_q(t) = \langle S^z_q(t) S^z_{-q}\rangle_{\mathrm{eq}} \tag{21}$$

$$= \frac{1}{L}\sum_{l=1}^{L}\sum_{l'=1}^{L} e^{iql} e^{-iql'} C_{l,l'}(t) \ , \tag{22}$$

where the discrete momenta take on the values $q = 2\pi\nu/L$ with $\nu = 0, 1, \ldots, L-1$. Eventually, another Fourier transform from the time to the frequency domain yields the so-called dynamical structure factor,

$$C_q(\omega) = \int_{-\infty}^{\infty} e^{i\omega t} C_q(t)\ \mathrm{d}t \ . \tag{23}$$

Let us note that $C_q(\omega)$ is proportional to the scattering cross section measured in inelastic neutron scattering experiments on, e.g., magnetic Mott insulator compounds (see Ref. [55] for a comparison between experiment and theory). This link between real-world experiments and the theoretical framework of equilibrium correlation functions highlights the significance of linear response theory.

A central aspect of this dissertation is to study the transport properties for a variety of low-dimensional quantum spin models within linear response theory. In particular, it is demonstrated that the combined analysis of the current autocorrelations $\langle j(t)j\rangle_{\mathrm{eq}}$ and the spatio-temporal correlations $C_{l,l'}(t)$ provides a comprehensive picture at all scales and allows to extract quantitative values of the transport coefficients.

Transport in the XXZ chain and the impact of integrability

As discussed in Sec. II.A, integrable models are characterized by a macroscopic number of (quasi) local conservation laws. These conservation laws can have an impact on the transport properties, i.e., they can protect currents from decaying. This can be conveniently exemplified for the case of the spin-1/2 XXZ chain (3). To begin with, let us consider energy transport in this model. Analogous to the continuity equation (15), it is possible to define the energy-current operator j_E, which takes on the form [52, 57]

$$j_E = J^2 \sum_{l=1}^{L} \big[\big(S^x_l S^y_{l+2} - S^y_l S^x_{l+2} \big) S^z_{l+1} - \Delta \big(S^x_l S^y_{l+1} - S^y_l S^x_{l+1} \big) \big(S^z_{l-1} + S^z_{l+2} \big) \big] \ . \tag{24}$$

As it turns out [57], j_E is itself a conserved quantity and commutes exactly with $\mathcal{H}_{\mathrm{XXZ}}$ for all anisotropies Δ. Thus, the correlation function $\langle j_E(t) j_E\rangle_{\mathrm{eq}}$ is time-independent and energy transport in the XXZ chain is ballistic at all temperatures.

More complicated is the case of spin transport. Here, the current operator j in Eq. (16) commutes with $\mathcal{H}_{\mathrm{XXZ}}$ only for $\Delta = 0$, i.e., in the case of free fermions. In contrast, for all $\Delta \neq 0$, one finds $[j, \mathcal{H}_{\mathrm{XXZ}}] \neq 0$, and $\langle j(t)j\rangle_{\mathrm{eq}}$ can in principle decay. In particular, the long-time average of $\langle j(t)j\rangle_{\mathrm{eq}}$ can be bounded from below by means of the Mazur inequality [56],

$$\lim_{\tau\to\infty} \frac{1}{\tau}\int_0^\tau \langle j(t)j\rangle_{\mathrm{eq}}\ \mathrm{d}t \geq \sum_m \frac{(j, Q_m)^2}{(Q_m, Q_m)} \ , \tag{25}$$

where the sum runs over a subset of orthogonal conserved quantities Q_m, with $(A, B) = \mathrm{Tr}[A^\dagger B]/d$ denoting the Hilbert-Schmidt inner product. The left hand side of Eq. (25), i.e., the (potentially) nondecaying part of the current-current correlation function, is often referred to as the Drude weight [52]. Note that a finite Drude weight directly implies ballistic

transport (within LRT). At zero magnetization (i.e. in the absence of a magnetic field), it has been realized that the spin and the energy current are orthogonal, $(j, j_E) = 0$, such that Eq. (25) with $Q_m = j_E$ cannot be used to infer that spin transport is ballistic [57]. Later, however, a nonzero Drude weight has been rigorously established for anisotropies $|\Delta| < 1$ thanks to a new class of quasi local conservation laws [58, 59], confirming numerical studies in this parameter regime [60].

In contrast, for larger anisotropies $\Delta > 1$, the spin Drude weight is expected to vanish and clean diffusive transport has been numerically observed at high temperatures [61, 62, 63]. Thus, while diffusion is generally not expected to occur in integrable models due to the extensive number of conservation laws, it is worth noting that integrability as such apparently does not rule out the possibility of diffusion.

Eventually, at the isotropic point $\Delta = 1$, the nature of spin transport has been the most controversial. Based on a number of recent works [64, 65], it is now widely accepted that high-temperature spin transport is superdiffusive at $\Delta = 1$. In this thesis, we provide further numerical evidence for the occurrence of superdiffusion by analyzing the time dependence of the diffusion coefficient $D(t)$ (see Sec. III.C for details).

C. Thermalization in isolated quantum systems

What is thermalization?

Consider a quantum many-body system $\mathcal{H}$, which is weakly coupled to a macroscopically large heat bath at temperature $T = 1/\beta$. Textbook quantum statistical mechanics asserts that, after a sufficiently long time, the state of the quantum system can be described by a canonical density matrix of Gibbs form,

$$\rho_{\mathrm{eq}} = \frac{e^{-\beta\mathcal{H}}}{\mathrm{Tr}[e^{-\beta\mathcal{H}}]} \ . \tag{26}$$

However, this thesis is concerned with the question whether and in which way an *isolated* quantum many-body system can approach thermal equilibrium, i.e., without invoking an additional external reservoir. To this end, let $\rho(0)$ be a (mixed or pure) out-of-equilibrium initial state. In an isolated system, the time evolution is unitary such that the state at time t is given by

$$\rho(t) = e^{-i\mathcal{H}t}\rho(0)e^{i\mathcal{H}t} \ . \tag{27}$$

Clearly, $\rho(t)$ will generally be different from ρ_{eq}, even at very long times. While the unitary time evolution (27) preserves information about the specific initial state $\rho(0)$, the equilibrium density matrix ρ_{eq} only depends on the inverse temperature $\beta = 1/T$ and on the Hamiltonian $\mathcal{H}$. This becomes even more obvious if $\rho(0) = |\psi(0)\rangle\langle\psi(0)|$ is a pure state. Under unitary time evolution, a pure state will always remain pure (i.e. the von Neumann entropy of $\rho(t)$ is time-independent), whereas ρ_{eq} is a mixed maximum-entropy state.

While it is hard to understand thermalization based on the state $\rho(t)$ of the *full* isolated system, an important insight is to consider *subsystems* instead [74]. Namely, an isolated quantum system is called *thermal*, if it is able to act as a heat bath for all its subsystems [74]. To be precise, let the whole system be subdivided into a part A which comprises only a small fraction of the total number of degrees of freedom, and a larger part B which contains the rest of the system. The reduced density matrix of $\rho(t)$ on the subsystem A then follows by tracing out the degrees of freedom in B,

$$\rho_A(t) = \mathrm{Tr}_B[\rho(t)] \ . \tag{28}$$

The system is said to thermalize if, in the long-time and large-system limit, the reduced density matrix $\rho_A(t)$ approaches a thermal equilibrium state [74],

$$\lim_{t\to\infty}\lim_{L\to\infty} \rho_A(t) = \mathrm{Tr}_B[\rho_{\mathrm{eq}}] \ , \tag{29}$$

where the temperature of ρ_{eq} is fixed by the energy density of the initial state $\rho(0)$. If Eq. (29) applies, then the measurements of local observables agree with the appropriate thermodynamic ensemble average. Note that in contrast to $\rho(t)$, the von Neumann entropy of $\rho_A(t)$ can increase due to the buildup of entanglement with the environment B (see also Fig. 10 of Ref. [R1]). While Eq. (29) can be used to define what it means for an isolated quantum system to thermalize, this definition is somewhat impractical. Therefore, in the following, the time-dependent relaxation process towards thermal equilibrium is discussed from another perspective.

The eigenstate thermalization hypothesis (ETH)

Instead of studying the time evolution of the system's state $\rho(t)$, it is instructive to consider the expectation-value dynamics of physical operators $\mathcal{O}$,

$$\langle\mathcal{O}(t)\rangle = \mathrm{Tr}[\rho(t)\mathcal{O}] \ . \tag{30}$$

In contrast to the correlation function (14), the subscript "eq" has been omitted in Eq. (30) to indicate that $\langle\mathcal{O}(t)\rangle$ is a nonequilibrium expectation value. Let $\rho(0) = |\psi(0)\rangle\langle\psi(0)|$ now be a pure (out-of-equilibrium) state written in terms of the eigenstates $|n\rangle$ of the underlying Hamiltonian $\mathcal{H}$, i.e.,

$$|\psi(0)\rangle = \sum_{n=1}^{d} c_n |n\rangle \ , \tag{31}$$

where the coefficients $c_n = \langle n|\psi(0)\rangle$ denote the overlap between $|\psi(0)\rangle$ and $|n\rangle$, and d is the dimension

of the Hilbert space. (While pure states are considered here for reasons of simplicity, it is straightforward to generalize the following discussion also to mixed states [13].) Moreover, let $|\psi(0)\rangle$ have an average energy $\bar{E} = \sum_n |c_n|^2 E_n$ (where E_n are the eigenvalues of $\mathcal{H}$), with energy fluctuations

$$\delta E = \sqrt{\langle\psi(0)|\,\mathcal{H}^2\,|\psi(0)\rangle - \bar{E}^2}\ , \tag{32}$$

that are macroscopically small compared to the full spectrum of $\mathcal{H}$. In the eigenbasis of $\mathcal{H}$, the time evolution of $|\psi(t)\rangle$ becomes,

$$|\psi(t)\rangle = \sum_{n=1}^{d} c_n e^{-iE_n t}\,|n\rangle\ , \tag{33}$$

where each of the coefficients c_n simply acquires an additional phase determined by the corresponding eigenvalue E_n. Given $|\psi(t)\rangle$, the out-of-equilibrium dynamics $\langle\mathcal{O}(t)\rangle$ in Eq. (30) can be written as [13]

$$\begin{aligned}\langle\mathcal{O}(t)\rangle &= \langle\psi(t)|\,\mathcal{O}\,|\psi(t)\rangle \qquad (34)\\ &= \sum_{n=1}^{d} |c_n|^2\mathcal{O}_{nn} + \sum_{\substack{m,n=1\\ m\neq n}}^{d} c_m^* c_n e^{i(E_m-E_n)t}\mathcal{O}_{mn}\ ,\end{aligned}$$

where $\mathcal{O}_{mn} = \langle m|\mathcal{O}|n\rangle$ are the matrix elements of $\mathcal{O}$ in the eigenbasis of $\mathcal{H}$. Assuming the absence of degenerate energy gaps, the long-time average of $\langle\mathcal{O}(t)\rangle$ then follows as

$$\overline{\mathcal{O}} = \lim_{\tau\to\infty}\frac{1}{\tau}\int_0^\tau \langle\mathcal{O}(t)\rangle\ \mathrm{d}t = \sum_{n=1}^{d}|c_n|^2\mathcal{O}_{nn}\ , \tag{35}$$

since the off-diagonal terms in Eq. (34) dephase at long times and vanish upon taking the time average. Thus, one can think of $\overline{\mathcal{O}}$ as the prediction of a *diagonal ensemble* [31], i.e., $\overline{\mathcal{O}} = \mathrm{Tr}[\mathcal{O}\rho_{\mathrm{de}}]$ with $\rho_{\mathrm{de}} = \sum_n |c_n|^2\,|n\rangle\langle n|$.

As a first criterion for thermalization, it is natural to demand that the long-time value $\overline{\mathcal{O}}$ has to (approximately) agree with the microcanonical expectation value $\mathcal{O}_{\mathrm{mc}}$ at the corresponding energy density,

$$\overline{\mathcal{O}} \overset{!}{\approx} \mathcal{O}_{\mathrm{mc}}\ , \quad \text{with } \mathcal{O}_{\mathrm{mc}} = \frac{1}{N_{\bar{E}}}\sum_{m=1}^{N_{\bar{E}}}\mathcal{O}_{mm}\ , \tag{36}$$

where the sum runs over all $N_{\bar{E}}$ eigenstates $|m\rangle$ in the microcanonical energy window $E_m \in [\bar{E}-\delta E, \bar{E}+\delta E]$. Apparently, Eq. (36) is difficult to satisfy in general (i.e. for all initial states $|\psi(0)\rangle$) since $\overline{\mathcal{O}}$ explicitly depends on $|\psi(0)\rangle$ in terms of the (exponentially many) coefficients c_n, whereas $\mathcal{O}_{\mathrm{mc}}$ is fixed by the average energy $\bar{E}$. The eigenstate thermalization hypothesis provides a way to bridge this gap [29, 30, 31]. In particular, the ETH states that the diagonal matrix elements of local operators $\mathcal{O}_{nn}$ in the eigenbasis of generic (nonintegrable) Hamiltonians $\mathcal{H}$ are a smooth function of energy (with fluctuations that vanish for $L\to\infty$) and agree with $\mathcal{O}_{\mathrm{mc}}$. If this would be the case, then the $\mathcal{O}_{nn}$ in Eq. (35) can be pulled in front of the sum and, with proper normalization of the initial state, it follows that $\overline{\mathcal{O}} = \mathcal{O}_{\mathrm{mc}}$ [13]. In hindsight, this result can also be understood from the following thought experiment. If one requires thermalization for every possible initial state $|\psi(0)\rangle$, this should also hold for the special case of $|\psi(0)\rangle = |n\rangle$ being an exact eigenstate of $\mathcal{H}$. In this case, however, the expectation value of $\mathcal{O}$ becomes time independent, $\langle\mathcal{O}(t)\rangle = \langle\mathcal{O}(0)\rangle = \mathcal{O}_{nn}$. Thus, the individual state $|n\rangle$ already has to be thermal in order to fulfill Eq. (36).

So far, the ETH ensures agreement between $\overline{\mathcal{O}}$ and the microcanonical ensemble average. However, any practical definition of thermalization should furthermore require that the fluctuations $\sigma^2_{\mathcal{O}} = \overline{\langle\mathcal{O}(t)\rangle^2} - \overline{\mathcal{O}}^2$ around the long-time average are sufficiently small. It is rather straightforward to show that $\sigma^2_{\mathcal{O}}$ is controlled by the off-diagonal matrix elements of $\mathcal{O}$ [13],

$$\begin{aligned}\sigma^2_{\mathcal{O}} &= \lim_{\tau\to\infty}\frac{1}{\tau}\int_0^\tau \langle\mathcal{O}(t)\rangle^2\mathrm{d}t - \overline{\mathcal{O}}^2 \qquad (37)\\ &= \lim_{\tau\to\infty}\frac{1}{\tau}\int_0^\tau \sum_{m\neq n, p\neq q}\mathcal{O}_{mn}\mathcal{O}_{pq}c_m^* c_n c_p^* c_q \qquad (38)\\ &\qquad\qquad \times e^{i(E_m-E_n+E_p-E_q)t}\ \mathrm{d}t\\ &= \sum_{m,n\neq m}|c_m|^2|c_n|^2|\mathcal{O}_{mn}|^2 \leq \max\,|\mathcal{O}_{mn}|\ , \qquad (39)\end{aligned}$$

where it has been used from (38) to (39) that contributions only arise for the simultaneous index combination $m = q$ and $n = p$. Moreover, in (39), the $|\mathcal{O}_{mn}|^2$ have been bounded from above by their maximum and the normalization of $|\psi(0)\rangle$ has been used. Thus, in order to guarantee that $\langle\mathcal{O}(t)\rangle$ stays close to its average $\overline{\mathcal{O}}$ at almost all times, one has to demand that the off-diagonal elements $\mathcal{O}_{mn}$ are small.

Motivated by random-matrix theory, the following matrix representation for the diagonal and the off-diagonal part of local operators in the eigenbasis of generic Hamiltonians has been proposed [66],

$$\mathcal{O}_{mn} = \mathcal{F}_{\mathrm{d}}(\bar{E})\,\delta_{mn} + \Omega(\bar{E})^{-\frac{1}{2}}\,\mathcal{F}_{\mathrm{od}}(\bar{E},\omega_{mn})\,r_{mn}\ , \tag{40}$$

where $\bar{E} = (E_m+E_n)/2$ and $\omega_{mn} = E_m - E_n$. Here, the functions $\mathcal{F}_{\mathrm{d}}$ and $\mathcal{F}_{\mathrm{od}}$ depend smoothly on their arguments, with $\mathcal{F}_{\mathrm{d}}$ coinciding with the appropriate microcanonical expectation value at energy $\bar{E}$. The r_{mn} are random numbers (within the constraint of $r_{mn} = r_{nm}^*$), which are drawn from a Gaussian distribution with zero mean and unit variance. Moreover, these off-diagonal elements are weighted by $\Omega(\bar{E})^{-1/2}$, where $\Omega(\bar{E})$ is the density of states. Since $\Omega(\bar{E})$ grows exponentially in the size of the system, the fluctuations $\sigma^2_{\mathcal{O}}$ in (39) are strongly suppressed. The expression (40) is referred to as ETH ansatz.

The ETH ansatz (40) also plays an important role in the present thesis. Specifically, in Ref. [R6], we study the nonequilibrium dynamics resulting from a realistic class of out-of-equilibrium initial states. For these states, we particularly scrutinize the off-diagonal part of Eq. (40) and its impact on the full time-dependent relaxation process prior to thermalization. Moreover, in Ref. [R8], we are concerned with the question if the ETH is indeed a physically necessary condition for the occurrence of thermalization in realistic situations.

Breakdown of the ETH

While there is convincing numerical evidence that Eq. (40) holds for a number of systems and observables [67, 68, 69, 70], rigorous conditions for the validity of the ETH are still missing, i.e., the ETH is just an hypothesis. While it is believed to be valid for generic quantum many-body systems and local observables [13], there are also classes of systems where the ETH is clearly violated. The simplest example is the case of integrable models. As a consequence of their extensive number of conservation laws, integrable models are not expected to thermalize to standard statistical ensembles such as Eq. (26). Instead, it has been found that the long-time steady state in such systems can be captured in terms of a so-called generalized Gibbs ensemble [71], i.e., a maximum-entropy state with respect to the additional conserved quantities [72].

Recently, disordered models have attracted a vast amount of interest as another class of ETH-violating systems. For sufficiently strong disorder, it is believed that these models can undergo a transition from an ergodic phase where the ETH holds into a many-body localized regime where the ETH breaks down [73, 74, 75]. Many-body localization (MBL) generalizes the well-known phenomenon of Anderson localization to the presence of interactions and can be understood in terms of an emergent set of local integrals of motion [76, 77]. This emergent integrability of the MBL phase also reflects itself in the level-spacing distribution, which exhibits a crossover from Wigner-Dyson to Poissonian statistics upon increasing the disorder [78]. Connecting to the discussion in the context of Eq. (29), one can say that many-body localized systems fail to act as a heat bath for their subsystems. The transport properties of disordered systems and the eventual onset of many-body localization are studied in Refs. [R2] and [R9] of this thesis (see also Ref. [R11]).

D. Numerical methods for quantum many-body dynamics

This Section provides a brief introduction to the numerical methods which are employed in this thesis, namely, (i) *exact diagonalization*, (ii) *dynamical quantum typicality*, and (iii) *numerical linked cluster expansions*. It is important to note that this list is by no means exhaustive and that there exist a variety of other sophisticated methods to study the dynamics of quantum many-body systems. Examples include, e.g., quantum Monte Carlo methods [79] (see also Ref. [R9]), dynamical mean field theory [80], Krylov subspace techniques [81], as well as novel approaches based on machine learning [82]. Most notably, the time-dependent density matrix renormalization group, including related methods based on matrix product states, have proven to be powerful tools to study dynamical properties especially of one-dimensional models [32, 83]. Since each of these methods has its own specific strengths and drawbacks, it generally depends on the given physical problem which method is to be favored.

Exact diagonalization (ED)

Exact diagonalization is arguably the simplest approach to study the properties of quantum many-body systems. Given a finite dimensional Hamiltonian $\mathcal{H}$, the main idea of ED is to obtain all eigenvalues E_n and eigenstates $|n\rangle$ which satisfy $\mathcal{H}\,|n\rangle = E_n\,|n\rangle$. The knowledge of the E_n and $|n\rangle$ then allows to calculate all static and dynamical properties. For instance, the current autocorrelation function $\langle j(t)j\rangle_{\text{eq}}$ in Eq. (14) can be written in a spectral representation,

$$\langle j(t)j\rangle_{\text{eq}} = \sum_{m,n=1}^{d} \frac{e^{-\beta E_m}}{\mathcal{Z}} e^{i(E_m-E_n)t} |\langle m|\, j\, |n\rangle|^2 \;, \quad (41)$$

which can be evaluated for arbitrary time scales and temperatures. Likewise, the out-of-equilibrium dynamics $\langle \mathcal{O}(t)\rangle$ in Eq. (34) can be calculated for every initial state $|\psi(0)\rangle$ and observable $\mathcal{O}$.

However, since the Hilbert-space dimension of a quantum many-body system grows exponentially in the number of degrees of freedom, ED is generally limited to rather small system sizes. As an example, consider a spin-1/2 chain of length $L = 20$, where the Hilbert space has dimension $d = 2^{20} \approx 10^6$. Storing the full matrix representation of $\mathcal{H}$ (with double precision) would require approximately 8.8 TB of memory, which is clearly out of reach for standard workstations. In practice, these enormous memory requirements can be (at least partially) mitigated by exploiting the symmetries of the Hamiltonian such as, e.g., the conservation of the total magnetization S^z, cf. Eq. (12). In this case, the Hamiltonian can be decomposed into smaller blocks which are solved separately [84]. However, despite exploiting this and other symmetries, the calculation of (static and dynamical) properties [e.g. Eq. (41)] by means of full ED is limited to spin-1/2 systems of size $L \approx 20$. Since such system sizes are often too small to correctly describe the physical

properties in the thermodynamic limit $L \to \infty$, the exponential memory requirements are a serious drawback of ED (not to mention the scaling of the runtime with L).

Nevertheless, the importance of ED should not be underestimated. On the one hand, ED of small systems is an indispensable tool to check the correctness of results obtained by other more sophisticated methods. On the other hand, there can be situations where ED is the only numerical method applicable. For instance, in the context of thermalization, ED gives direct access to the individual matrix elements $\mathcal{O}_{mn}$, which is crucial to study the ETH ansatz (40).

Dynamical quantum typicality (DQT)

Loosely speaking, the concept of typicality states that a single pure quantum state can imitate the full statistical ensemble. In this context, typicality has been put forward as an important building block to explain the emergence of thermodynamic behavior [25]. For instance, it is a central result of typicality that for the overwhelming majority of pure states drawn from a narrow energy shell, the reduced density matrix for a small subsystem is essentially the canonical equilibrium state [26, 27]. Or to put it differently, nonequilibrium quantum states are mathematically rare.

Interestingly, it has been shown that the concept of typicality also carries over to the dynamics of quantum expectation values (see also Ref. [R7] of this thesis). Quoting from Ref. [85], dynamical quantum typicality describes the fact that *"the vast majority of all pure states featuring a common expectation value of some generic observable at a given time will yield very similar expectation values of the same observable at any later time"*. Moreover, typicality arguments (also for observables) have been successfully employed to predict the entire temporal relaxation process for some quantum many-body systems out of equilibrium [34]. A more detailed presentation of the conceptual aspects of (dynamical) quantum typicality can be found in, e.g., Ref. [25].

It is the aim of this Section to discuss how the concept of DQT can be exploited as an efficient numerical approach to quantum many-body dynamics. To this end, let us again consider the current autocorrelation function $\langle j(t)j\rangle_{\text{eq}}$. From a practical perspective, the main idea of DQT is to replace the trace over the full many-body basis [cf. Eq. (14)] by a scalar product with a single "typical" pure state. Specifically, $\langle j(t)j\rangle_{\text{eq}}$ can be rewritten according to [86, 87, 88],

$$\langle j(t)j\rangle_{\text{eq}} = \frac{\langle\psi_\beta(t)|\, j\, |\varphi_\beta(t)\rangle}{\langle\psi_\beta(0)|\psi_\beta(0)\rangle} + \epsilon \ , \tag{42}$$

where ϵ is a statistical error (see discussion further below), and the two auxiliary pure states $|\psi_\beta(t)\rangle$ and $|\varphi_\beta(t)\rangle$ are given by

$$|\psi_\beta(t)\rangle = e^{-i\mathcal{H}t}e^{-\beta\mathcal{H}/2}\,|\psi\rangle \ , \tag{43}$$

$$|\varphi_\beta(t)\rangle = e^{-i\mathcal{H}t}j\ e^{-\beta\mathcal{H}/2}\,|\psi\rangle \ , \tag{44}$$

with the reference pure state $|\psi\rangle$ being constructed as

$$|\psi\rangle = \sum_{k=1}^{d} c_k\,|k\rangle \ . \tag{45}$$

Here, the real and imaginary parts of the complex coefficients c_k are drawn at random from a Gaussian distribution with zero mean, and the states $|k\rangle$ can denote any orthogonal basis of the Hilbert space with dimension d. In practice, a natural choice is the common eigenbasis of the local S_l^z operators (also known as the Ising basis), i.e., basis states of the form $|\uparrow\downarrow\downarrow\cdots\rangle$, $|\uparrow\downarrow\uparrow\cdots\rangle$, ... and so forth.

Since $|\psi\rangle$ is a random vector, the error ϵ in Eq. (42) is a random variable as well. However, it is the important insight of typicality that the standard deviation of ϵ scales as $\sigma(\epsilon) \propto 1/\sqrt{d_{\text{eff}}}$, where $d_{\text{eff}} = \text{Tr}\{\exp[-\beta(H-E_0)]\}$ is the effective dimension of the Hilbert space and E_0 is the ground-state energy of $\mathcal{H}$, i.e., d_{eff} is essentially the number of thermally occupied states. (For rigorous error bounds see, e.g., Refs. [85, 89, 90].) Thus, in the high-temperature limit $\beta \to 0$, one has $d_{\text{eff}} = d$, and $\sigma(\epsilon)$ decreases exponentially upon increasing the system size L (recall that $d = 2^L$ for spin-1/2 systems). Actually, $\sigma(\epsilon)$ decreases exponentially with L also at finite temperatures $\beta > 0$, albeit slower compared to $\beta = 0$. In any case, the accuracy of the typicality approach can be further improved by averaging nominator and denominator of Eq. (42) over a set of independently drawn random states [86]. Especially for $\beta = 0$, however, such an averaging often turns out to be unnecessary, and a single pure state $|\psi\rangle$ is enough to accurately reproduce the exact equilibrium correlation function $\langle j(t)j\rangle_{\text{eq}}$.

Eventually, let us note that analogous constructions as in Eq. (42) are possible also for other equilibrium correlation functions such as $C_{l,l'}(t)$ in Eq. (20). Moreover, typical pure states allow to accurately approximate time-dependent expectation values $\langle\mathcal{O}(t)\rangle$ [cf. Eq. (30)] for specific out-of-equilibrium initial states as well (see Sec. III.B).

The main numerical advantage of DQT comes from the fact that the matrix exponentials $e^{-\beta\mathcal{H}/2}$ and $e^{-i\mathcal{H}t}$ can be efficiently applied to pure quantum states by iteratively solving the Schrödinger equation in imaginary and real time, respectively. Specifically, given the state $|\psi_\beta(t)\rangle$ in Eq. (43) at some time t, its time-evolved counterpart at time $t+\delta t$ is formally given by

$$|\psi_\beta(t+\delta t)\rangle = e^{-i\mathcal{H}\delta t}\,|\psi_\beta(t)\rangle \ , \tag{46}$$

where δt is a small discrete time step. While the exact evaluation of Eq. (46) would require the full diag-

onalization of $\mathcal{H}$, there exist a variety of approximation schemes which circumvent the necessity of ED. A particular simple approach in this context is a fourth-order Runge-Kutta (RK4) method which, in the case of Eq. (46), simply reduces to a Taylor expansion of the exponential $e^{-i\mathcal{H}\delta t}$ [87, 88],

$$|\psi_\beta(t+\delta t)\rangle \approx |\psi_\beta(t)\rangle + \sum_{n=1}^{4} \frac{(-i\mathcal{H}\delta t)^n}{n!} |\psi_\beta(t)\rangle \ . \quad (47)$$

Completely analogous, the temperature dependence of $|\psi_\beta(0)\rangle$ can be generated by a Taylor expansion of $e^{-\beta\mathcal{H}/2}$. Importantly, the RK4 scheme (47) boils down to the calculation of matrix-vector products, which can be carried out comparatively memory efficient. Namely, the memory requirements are essentially set by the size of a few vectors and by the Hamiltonian $\mathcal{H}$. For local interactions, $\mathcal{H}$ typically has a very sparse matrix structure and can either be kept in memory as well, or its matrix elements can be calculated *on-the-fly* when they are needed. Since the time and the memory requirements only grow linearly in the dimension of the Hilbert space [87, 91], correlation functions such as $\langle j(t)j\rangle_{\rm eq}$ can be evaluated for system sizes and Hilbert-space dimensions substantially larger compared to ED.

Note that while the RK4 scheme (47) yields very accurate results if δt is sufficiently small [88], it violates the underlying unitarity of the original time evolution (46). This shortcoming of RK4 is cured by more sophisticated approaches such as, e.g., Trotter decompositions [91], Chebyshev polynomials [92, 93], as well as Krylov subspace techniques [94]. Analogous to RK4, a unifying feature of all these methods is that they require the successive calculation of matrix-vector products. However, since unitarity is preserved, these methods can typically tolerate a larger time step δt while maintaining a high accuracy [92].

Numerical linked cluster expansions (NLCE)

In comparison to ED and DQT, numerical linked cluster expansions provide a means to study quantum many-body systems directly in the thermodynamic limit. Originally, NLCE have been introduced to study thermodynamic properties such as the specific heat or the entropy for a variety a lattice models [95]. (For a review of NLCE, see also Ref. [96].) Recently, NLCE have been successfully employed to access the time evolution of observables resulting from quantum quench protocols [97]. Here, let us discuss that NLCE also yield an efficient method to calculate time-dependent correlation functions.

Within NLCE, the value of an extensive quantity per lattice site is calculated in the thermodynamic limit as the sum of contributions from all connected clusters which can be embedded on the lattice. The notion of connected cluster here refers to a finite number of lattice sites which are coupled by the respective Hamiltonian. Moreover, the contribution of each cluster within the NLCE is evaluated numerical exact, e.g., by means of ED. This is in contrast to related high-temperature expansions, where extensive quantities are perturbatively expanded in powers of the inverse temperature [98]. As a consequence, NLCE can yield converged results at considerably lower temperatures.

To illustrate the basic idea of NLCE, let us once again consider the (extensive) current autocorrelation function $\langle j(t)j\rangle_{\rm eq}$, which is expanded according to

$$\langle j(t)j\rangle_{\rm eq}/L = \sum_c \mathcal{L}_c W_c(t) \ , \quad (48)$$

where the sum runs over all clusters c with multiplicity $\mathcal{L}_c$, i.e., $\mathcal{L}_c$ is the number of ways (per site) the cluster c can be embedded on the lattice. Moreover, the weight $W_c(t)$ of a given cluster c is calculated using the inclusion-exclusion principle,

$$W_c(t) = \langle j(t)j\rangle_{\rm eq}^{(c)} - \sum_{s\subset c} W_s(t) \ , \quad (49)$$

where the weight $W_s(t)$ of all subclusters s of c is subtracted, and $\langle j(t)j\rangle_{\rm eq}^{(c)}$ denotes the current autocorrelation function evaluated on the cluster c.

If all clusters are considered, then Eq. (48) by construction yields the exact result for the quantity of interest. However, for a given arbitrary lattice geometry, the identification of all linked clusters (including their multiplicities) can become a very difficult combinatorial problem. Specifically, the number of different clusters comprising a fixed number of lattice sites N typically grows exponentially with N. (Note that for one-dimensional systems, the identification of clusters becomes considerably simpler, see Sec. III.C.) Importantly, evaluating the weights in Eq. (49) by means of ED is only feasible for small to intermediate sized clusters. As a consequence, the sum in Eq. (48) eventually has to be truncated to a maximum cluster size $c_{\rm max}$ which can be treated numerically. Thus, while the NLCE yields results in the thermodynamic limit and a finite-size scaling becomes in principle unnecessary, one has to check the convergence of the NLCE depending on the chosen cutoff $c_{\rm max}$ [96]. Typically, a larger $c_{\rm max}$ extends the convergence down to lower temperatures (for thermodynamic quantities) [96], or up to longer times (for time-dependent quantities) [97]. In this thesis, we demonstrate that $c_{\rm max}$ can be significantly increased by combining NLCE with dynamical quantum typicality.

III. GUIDE TO PUBLICATIONS

In the following, an overview of the scope and the main results of Refs. [R1] - [R10] is given. To this

end, the papers have been grouped into the three categories (i) *Transport and the emergence of diffusion in quantum models* (Sec. III.A), (ii) *Nonequilibrium dynamics close to and far away from equilibrium* (Sec. III.B), and (iii) *Development of numerical and (semi-)analytical approaches* (Sec. III.C). Each of the Secs. III.A - III.C starts by presenting the main results of the corresponding papers and by discussing the relationships of the works among each other. Subsequently, a brief individual summary of each paper is provided, including additional comments on findings beyond the main results. While Secs. III.A - III.C already contain some technical details, they should be self-contained and comprehensible in view of the previous Sec. II. For a more detailed discussion, we refer to the original works [R1] - [R10].

A. Transport and the emergence of diffusion in quantum models [R1, R5, R9]

Integrability is rather the exception than the rule and can be broken in numerous ways. While integrable models can (but do not need to) exhibit ballistic transport (see Sec. II.B), one might expect that for more generic (nonintegrable) models, normal diffusive behavior emerges, e.g., due to quantum chaos [99]. Still, in view of the multitude of different integrability-breaking perturbations, it is an open question if diffusion is indeed a generic feature for the majority of nonintegrable models (note that counterexamples have been proposed [100]). To work towards an answer of this question, Refs. [R1], [R5] and [R9], study the infinite-temperature transport properties for a variety of (quasi) one-dimensional spin models within linear response theory.

Specifically, we take into account three different mechanisms to break the integrability of the XXZ chain. Namely, (i) an additional next-nearest neighbor interaction, (ii) couplings between separate chains, and (iii) a higher spin quantum number $S = 1$. As a main result, it is shown in Refs. [R1, R5, R9] that diffusive transport occurs for all integrability-breaking perturbations considered (see the detailed discussion of [R9] below for a possible exception). Our numerical analysis is based on looking at different signatures in real and momentum space as well as in the time and the frequency domain, which can all be equally well detected.

First, we study the spatio-temporal correlation functions $C_{l,l'}(t)$ introduced in Eq. (20). At infinite temperature, different lattice sites are uncorrelated initially, and the $C_{l,l'}(t)$ realize a δ-peak profile at time $t = 0$,

$$C_{l,l'}(t=0) = \begin{cases} \chi, & l = l' \\ 0, & l \neq l' \end{cases} , \tag{50}$$

with the susceptibility $\chi = 1/4$ at $\beta = 0$ and $S = 1/2$. The build-up of correlations for times $t > 0$, i.e., the broadening of this initial δ peak then serves as a diagnostic of the transport properties. The onset of diffusive transport reflects itself in a Gaussian broadening of the δ peak,

$$C_{l,l'}(t) \propto \exp\left[-\frac{(l-l')^2}{2\Sigma(t)^2}\right] , \tag{51}$$

which is observed in [R1], [R5], and [R9] with high accuracy. In particular, the width of the Gaussians is found to grow as

$$\Sigma(t) \propto \sqrt{t} . \tag{52}$$

As a consequence of this Gaussian broadening, the equal-site correlation function $C_{l,l'=l}(t)$ exhibits a distinct power-law decay [R9],

$$\langle S^z_l(t) S^z_l \rangle_{\rm eq} \propto t^{-1/2} . \tag{53}$$

In addition to the real-space correlations, we also analyze the transport properties in momentum space. In the long-wavelength limit, i.e., for sufficiently small momenta q, we find that the intermediate structure factor $C_q(t)$ [cf. Eq. (21)] decays exponentially,

$$C_q(t) \propto e^{-\tilde{q}^2 D t} , \tag{54}$$

where $\tilde{q}^2 = 2[1 - \cos(q)]$. In direct correspondence to this exponential decay, the dynamical structure factor $C_q(\omega)$ [cf. Eq. (23)] can be accurately described by Lorentzians at such small q,

$$C_q(\omega) \propto \frac{1}{\omega^2 + \tilde{q}^4 D^2} . \tag{55}$$

The combined analysis of the signatures (51) - (55) provides a comprehensive picture of the transport properties and, at least for the integrability-breaking perturbations considered by us, nicely confirms the emergence of diffusion in these models.

From a practical perspective, it is moreover demonstrated in Refs. [R1], [R5], and [R9] that dynamical quantum typicality provides an efficient means to study the spatio-temporal correlations $C_{l,l'}(t)$ (as well as the current autocorrelations $\langle j(t) j \rangle_{\rm eq}$) for long time scales and comparatively large system sizes (up to $L = 40$, i.e., $d = 2^{40}$ in [R5]).

Ref. [R1]: *"Real-time dynamics of typical and untypical states in nonintegrable systems"*

In Ref. [R1], the spin-1/2 XXZ chain (3) is studied in the presence of an additional next-nearest neighbor interaction of strength Δ', i.e., the total Hamiltonian $\mathcal{H}$ reads

$$\mathcal{H} = \mathcal{H}_{\rm XXZ} + J\Delta' \sum_{l=1}^{L} S^z_l S^z_{l+2} . \tag{56}$$

For this model, we analyze the real-time dynamics of local magnetization densities, $\langle S_l^z(t)\rangle$, resulting from a convenient class of nonequilibrium states $|\psi(0)\rangle$ which feature a sharp initial density profile. Specifically, the states $|\psi(0)\rangle$ are constructed as a superposition of all Ising-basis states $|k\rangle$ with a spin-up state in the center of the chain, i.e.,

$$|\psi(0)\rangle = \mathcal{P}_{L/2} \sum_{k=1}^{2^L} c_k |k\rangle \ , \quad \mathcal{P}_{L/2} = S_{L/2}^z + \frac{1}{2} \ , \quad (57)$$

where the c_k are chosen to be either random, partially random, or nonrandom. Since this class of initial states allows for changing internal degrees of freedom (e.g. the amount of randomness of the coefficients c_k) without modifying the initial density profile, we are able to investigate whether and in how far such internal details influence the real-time broadening.

On the one hand, in the case of high internal randomness (i.e. Gaussian distributed c_k), it is shown that the out-of-equilibrium dynamics $\langle S_l^z(t)\rangle$ can be related to the spatio-temporal correlation functions $C_{l,l'}(t)$ by means of dynamical quantum typicality (see also [101]), which enables us to study transport in the framework of LRT. For strong interactions ($\Delta, \Delta' > 1$), signatures of diffusion, e.g., Gaussian density profiles, are found to be of equal quality compared to earlier studies of the bare integrable XXZ chain [101]. Moreover, for weaker interactions ($\Delta, \Delta' < 1$), we demonstrate that diffusive transport emerges as long as integrability is broken.

On the other hand, for the specific choice of all c_k being the same, $|\psi(0)\rangle$ can be written as an unentangled product state with a spin-up state $|\uparrow\rangle$ in the middle of the chain and a spin-up/spin-down superposition at all other sites [101],

$$|\psi(0)\rangle \propto \ldots (|\uparrow\rangle + |\downarrow\rangle) \otimes |\uparrow\rangle \otimes (|\uparrow\rangle + |\downarrow\rangle) \ldots \ . \quad (58)$$

Although the density profiles are not distinguishable at $t = 0$, the dynamics for times $t > 0$ is found to strongly depend on whether $|\psi(0)\rangle$ is a "typical" state with random c_k or this "untypical" state where all c_k are the same (see also [101]).

In Ref. [R1], we provide an explanation of this difference by analyzing the local density of states and the entanglement of $|\psi(0)\rangle$. Note that, in contrast to the product state (58), $|\psi(0)\rangle$ is almost maximally entangled for random c_k [102]. In a nutshell, our results suggest that different initial conditions lead to the same dynamical behavior if their local density of states is similar. The initial entanglement entropy, on the other hand, does not seem to be a crucial property.

Ref. [R5]: *"Magnetization and energy dynamics in spin ladders: Evidence of diffusion in time, frequency, position, and momentum"*

In Ref. [R5], we consider a quasi one-dimensional spin-1/2 Heisenberg ladder described by the Hamiltonian $\mathcal{H} = \sum_{l=1}^{L} h_l$,

$$h_l = J_{||} \sum_{k=1}^{2} \mathbf{S}_{l,k} \cdot \mathbf{S}_{l+1,k} + \frac{J_\perp}{2} \sum_{n=l}^{l+1} \mathbf{S}_{n,1} \cdot \mathbf{S}_{n,2} \ , \quad (59)$$

where $J_{||}$ ($J_\perp$) denotes the coupling on the legs (rungs). Note that $\mathcal{H}$ decouples into two integrable Heisenberg chains for $J_\perp = 0$, whereas integrability is broken for any $J_\perp \neq 0$.

While the focus of [R5] is on the isotropic model with $J_\perp = J_{||}$, we show that the signatures (51) - (55) of spin diffusion can be detected for a variety of coupling ratios $J_\perp/J_{||}$, as well as in the presence of an additional magnetic field. Moreover, it is demonstrated that energy transport in the spin ladder (59) is diffusive as well.

As another interesting result, it is shown in Ref. [R5] that the structure factor $C_q(t)$ in the short-wavelength limit $q = \pi$ can be understood from a memory-kernel approach [103]. In this approach, the exactly solvable XX chain is chosen as a point of reference, where $C_\pi(t)$ is known to be described by a Bessel function [54]. This Bessel function is then interpreted as being generated by an integro-differential equation comprising a memory kernel $K(t)$. The additional rung couplings and zz terms in the spin ladder (59) are effectively treated as a perturbation which gives rise to an exponential damping of $K(t)$. In Ref. [R5], we find that the dynamics generated from this damped memory kernel agrees very well with the exact $C_\pi(t)$ of the spin ladder. The good agreement can not only be observed in real time, but also for the dynamical structure factor $C_\pi(\omega)$ in the frequency domain.

Ref. [R9]: *"Magnetization dynamics in clean and disordered spin-1 XXZ chains"*

In Ref. [R9], the XXZ chain (3) is studied for a larger spin quantum number $S = 1$. While the spin-1/2 version is known to exhibit ballistic, superdiffusive, and diffusive spin transport depending on the value of the anisotropy (cf. Sec. II.B), it is an intriguing question if normal diffusion generically occurs (i.e. for all Δ) upon considering $S = 1$.

Studying the signatures (51) - (55), it is shown in Ref. [R9] that high-temperature spin transport in the $S = 1$ model is diffusive in the easy-axis regime $\Delta > 1$ (analogous to the spin-1/2 chain). Moreover, we provide evidence that the signatures (53) and (55) are not exclusively restricted to the infinite-temperature limit, but can persist at lower temperatures as well, where we complement our results by additional quantum Monte Carlo simulations of large systems.

In contrast, it is shown that in the case of an isotropic chain, the signatures of diffusion are much less pronounced or even entirely absent, which suggests the existence of superdiffusion despite the nonintegrability of the spin-1 chain. While this finding

is consistent with results from other works [104], it has also been argued that normal diffusive transport will eventually set in for larger system sizes and longer time scales [105].

In addition to the clean model, Ref. [R9] also studies the effect of disorder on the spin dynamics, i.e., the Hamiltonian is modified according to

$$\mathcal{H} = \mathcal{H}_{\mathrm{XXZ}} + J \sum_{l=1}^{L} h_l S_l^z \ , \tag{60}$$

where the on-site magnetic fields $h_l \in [-W, W]$ are drawn at random from a uniform distribution, with $W \geq 0$ setting the magnitude of disorder. For spin $S = 1/2$, the Hamiltonian (60) is a central model to study the disorder-driven transition between a thermal phase ($W < W_c$) and a many-body-localized regime ($W > W_c$), where W_c is a critical disorder strength [78]. Not least due to the higher computational requirements, the dynamics of disordered models with $S > 1/2$ has remained largely unexplored.

In [R9], we observe that sufficiently strong disorder in the spin-1 chain leads to a breakdown of diffusion. While we are unable to detect clean signatures of MBL (at least for the largest values of W considered by us), our results might be consistent with the presence of a subdiffusive regime (analogous to numerical observations for the spin-1/2 chain at low to intermediate disorder below the MBL transition [106]). While not being discussed in detail in this guide to publications, let us note that the effect of disorder has been studied by us in quantum spin chains with even larger $S = 3/2$ and in chains consisting of classical spins [R11].

B. Nonequilibrium dynamics close to and far away from equilibrium [R2, R3, R6, R7, R8]

While the ETH provides an explanation for the occurrence of thermalization at long times, much less is known about the full time-dependent relaxation process prior to equilibration. A central motivation of Refs. [R2], [R3], [R6], [R7] and [R8] is to study this route to equilibrium for a variety of nonequilibrium scenarios.

To begin with, in Refs. [R2], [R3], and [R6], we consider a quantum system $\mathcal{H}$ affected by an external static force of strength ε, which gives rise to an additional potential $\mathcal{O}$ (conjugated to the force) within the Hamiltonian. Moreover, let the system be (weakly) coupled to a large heat bath at temperature $T = 1/\beta$, such that at time $t = 0$ the system can be described by the thermal density matrix

$$\rho(0) = \frac{e^{-\beta(\mathcal{H}-\varepsilon\mathcal{O})}}{\mathrm{Tr}[e^{-\beta(\mathcal{H}-\varepsilon\mathcal{O})}]} \ . \tag{61}$$

By removing both, the heat bath and the external force, one can induce a nonequilibrium situation, where $\rho(0)$ is an out-of-equilibrium state of the remaining Hamiltonian $\mathcal{H}$, and evolves according to the von Neumann equation, $\rho(t) = e^{-i\mathcal{H}t}\rho(0)e^{i\mathcal{H}t}$. In particular, $\rho(0)$ can be prepared close to equilibrium (by a weak static force) or far away from equilibrium (by a strong static force).

On the one hand, for weak forces, it is clear that the resulting expectation-value dynamics $\langle\mathcal{O}(t)\rangle = \mathrm{Tr}[\mathcal{O}\rho(t)]$ is well described by linear response theory, i.e., $\langle\mathcal{O}(t)\rangle$ is given by a suitable Kubo correlation function [35]. In contrast, for strong forces beyond the LRT regime, the dynamics can in principle be manifold. As a main result, we unveil in [R2], [R3], and [R6] that for high temperatures and certain classes of operators $\mathcal{O}$, the relaxation process $\langle\mathcal{O}(t)\rangle$ can become independent of whether or not $\rho(0)$ is close to equilibrium. Specifically, the dynamics in this case is generated by a single correlation function, even for far-from-equilibrium situations.

To proceed, a different but related nonequilibrium protocol is studied in Ref. [R8]. Here, the system is initially prepared in thermal equilibrium, and out-of-equilibrium conditions are dynamically generated due to an external force acting for a limited time window. Similar to the previous situation considered in Refs. [R2, R3, R6], this protocol allows to compare the close-to-equilibrium regime where linear response theory holds, and the far-from-equilibrium regime where LRT is supposed to break down. More details on the protocol and the results of Ref. [R8] can be found in the individual summary below.

Concerning the numerical analysis, it is important to mention that the different nonequilibrium scenarios studied in Refs. [R2, R3, R6, R8] are amenable to the concept of dynamical quantum typicality. Specifically, the initial density matrix $\rho(0)$ can be approximated by means of a typical pure state $|\psi(0)\rangle$ which is constructed according to

$$|\psi(0)\rangle = \frac{\sqrt{\rho(0)}\,|\psi\rangle}{\sqrt{\langle\psi|\,\rho(0)\,|\psi\rangle}} \ , \tag{62}$$

where $|\psi\rangle$ is a random state drawn from the full Hilbert space, cf. Eq. (45).

In contrast to the specific nonequilibrium situations explored in Refs. [R2, R3, R6, R8], Ref. [R7] studies the question of thermalization from a more abstract point of view. Namely, Ref. [R7] extends the original dynamical typicality scenario from Ref. [85] and considers a class of out-of-equilibrium initial states which exhibit a fixed measurement statistics of several commuting observables. For more details, see the summary of [R7] below.

Ref. [R3]: *"Relation between far-from-equilibrium dynamics and equilibrium correlation functions for binary operators"*

While the preparation of the initial states (61) in principle does not require a specific type of observable, Ref. [R3] focuses on so-called binary operators, $\mathcal{O} = c_1(\mathcal{P} + c_2)$, where c_1 and c_2 are some real constants, and all eigenvalues of $\mathcal{P}$ are either 0 or 1, i.e., $\mathcal{P}^2 = \mathcal{P}$ describes a projection. Binary operators are, e.g., local fermionic occupation numbers [cf. Eq. (8)] and local energy densities in the isotropic Heisenberg spin-1/2 chain. (These two examples are considered in the numerical simulations in [R3].) Furthermore, while the initial states (61) can be studied for arbitrary $T = 1/\beta$, we here focus on the regime of high temperatures. Specifically, in the limit $\beta \to 0$ but $\beta\varepsilon > 0$, one has in good approximation $\rho \propto e^{\beta\varepsilon\mathcal{O}}$, i.e., the Hamiltonian becomes essentially irrelevant for the initial state. Note that the subsequent dynamics, on the contrary, significantly depends on $\mathcal{H}$.

In Ref. [R3], we show that for this choice of high temperatures and binary operators, the nonequilibrium dynamics $\langle\mathcal{O}(t)\rangle = \mathrm{Tr}[\mathcal{O}\rho(t)]$ is generated by a single correlation function evaluated exactly at equilibrium. In particular, this statement holds true also for states in the far-from-equilibrium limit, i.e., outside the "trivial" linear response regime. Our result can be understood as a direct consequence of the projection property $\mathcal{P}^2 = \mathcal{P}$, since the initial state $\rho \propto e^{\beta\varepsilon\mathcal{P}}$ can then be written as

$$\begin{aligned}\rho &\propto 1 + \beta\varepsilon\mathcal{P} + \tfrac{1}{2}\beta^2\varepsilon^2\mathcal{P}^2 + \tfrac{1}{6}\beta^3\varepsilon^3\mathcal{P}^3 + \ldots \\ &= 1 + (e^{\beta\varepsilon} - 1)\,\mathcal{P}\ . \end{aligned} \tag{63}$$

From Eq. (63), it follows that

$$\langle\mathcal{P}(t)\rangle = \frac{\langle\mathcal{P}\rangle_{\mathrm{eq}} + (e^{\beta\varepsilon} - 1)\langle\mathcal{P}(t)\mathcal{P}\rangle_{\mathrm{eq}}}{1 + (e^{\beta\varepsilon} - 1)\langle\mathcal{P}\rangle_{\mathrm{eq}}}\ , \tag{64}$$

where only $\langle\mathcal{P}(t)\mathcal{P}\rangle_{\mathrm{eq}}$ depends on time. Thus, the nonequilibrium dynamics of binary operators, $\langle\mathcal{O}(t)\rangle = c_1(\langle\mathcal{P}(t)\rangle + c_2)$, is generated by the equilibrium correlation function $\langle\mathcal{P}(t)\mathcal{P}\rangle_{\mathrm{eq}}$, irrespective of the strength of the external force ε.

Ref. [R2]: *"Sudden removal of a static force in a disordered system: Induced dynamics, thermalization, and transport"*

In Ref. [R2], the real-time dynamics $\langle n_l(t)\rangle$ of local occupation numbers is studied for a one-dimensional model of spinless fermions with quenched disorder,

$$\mathcal{H} = \mathcal{H}_{\mathrm{JW}} + J\sum_{l=1}^{L}\mu_l(n_l - \tfrac{1}{2})\ , \tag{65}$$

where $\mathcal{H}_{\mathrm{JW}}$ has been introduced in Eq. (9), and the on-site potentials μ_l are randomly drawn from a uniform distribution $\mu_l \in [-W, W]$. The Hamiltonian (65) (or its spin-chain counterpart) is believed to undergo a transition to a many-body localized phase for strong disorder (see also summary of Ref. [R9] in Sec. III.A).

As a follow-up result of our previous findings in Ref. [R3], we show that for initial states of the form (61), the induced dynamics $\langle n_l(t)\rangle$ is again given by a single correlation function at equilibrium, irrespective of the strength of the external force. In particular, this type of "universality" holds true in both, the ergodic phase for small disorder and the many-body localized regime for large disorder.

In Ref. [R2], two important consequences are discussed. First, the long-time expectation value of the local densities is uniquely determined by the fluctuations of their diagonal matrix elements in the energy eigenbasis. Thus, the validity of the eigenstate thermalization hypothesis is not only a sufficient but also a necessary condition for thermalization. Second, the real-time broadening of density profiles is always given by the current autocorrelation function at equilibrium via a generalized Einstein relation. Moreover, in the context of transport, we discuss the influence of disorder for large particle-particle interactions, where normal diffusion is known to occur in the disorder-free case. Our results suggest that normal diffusion is stable against weak disorder, while they are consistent with anomalous diffusion for stronger disorder below the localization transition.

Ref. [R6]: *"Impact of eigenstate thermalization on the route to equilibrium"*

In Refs. [R2] and [R3], we have found that for binary operators and high temperatures, the relaxation process of $\langle\mathcal{O}(t)\rangle$ can become independent of whether the initial state $\rho(0)$ in (61) is prepared close to or far away from equilibrium. It is the motivation of Ref. [R6] to generalize this finding to a wider class of operators.

Focusing again on high temperatures, we recall that $\rho(0)$ essentially takes on the form $\rho \propto \exp(\beta\varepsilon\mathcal{O})$, such that the expectation value $\langle\mathcal{O}(t)\rangle = \mathrm{Tr}[\mathcal{O}(t)\rho]$ can be written as

$$\langle\mathcal{O}(t)\rangle = \sum_{N=0}^{\infty}\alpha_N(\varepsilon)\mathrm{Tr}[\mathcal{O}(t)\mathcal{O}^N]\ , \tag{66}$$

where we have used a Taylor expansion of the exponential function, and the $\alpha_N(\varepsilon)$ are some ε-dependent coefficients. From Eq. (66), it becomes clear that the relaxation dynamics of $\langle\mathcal{O}(t)\rangle$ is determined by the correlation functions $\mathrm{Tr}[\mathcal{O}(t)\mathcal{O}^N]$ for all values of the exponent N.

As a central result, we show in Ref. [R6] that the correlations $\mathrm{Tr}[\mathcal{O}(t)\mathcal{O}^N]$ for $N = 1, 2, 3, \ldots$ approxi-

mately fulfill the property,

$$\mathrm{Tr}[\mathcal{O}(t)\mathcal{O}^N]\begin{cases}\propto \mathrm{Tr}[\mathcal{O}(t)\mathcal{O}]\,, & \text{odd } N\\ =0\,, & \text{even } N\end{cases}\,, \tag{67}$$

given certain conditions on the matrix representation of the operator $\mathcal{O}$. Obviously, if Eq. (67) holds, then the whole time dependence of $\langle\mathcal{O}(t)\rangle$ follows from the "standard" correlation function $\mathrm{Tr}[\mathcal{O}(t)\mathcal{O}]$, analogous to the findings for binary operators in [R2] and [R3].

In [R6], we demonstrate that the conditions on the operator $\mathcal{O}$ in order to fulfill Eq. (67) are closely related to the ETH ansatz (40). In addition to Eq. (40), we demand as a main ingredient that the off-diagonal function $\mathcal{F}_{\mathrm{od}}$ varies only slowly with the average energy $\bar{E}$. Moreover, $\mathcal{F}_{\mathrm{od}}$ has to fall of sufficiently quickly for larger energy differences $|\omega_{mn}|$. Interestingly, the diagonal elements $\mathcal{O}_{mm}$ do not need to be smooth functions of $\bar{E}$ as claimed by (40), and variations that are uncorrelated with the off-diagonal elements leave Eq. (67) valid. In Ref. [R6], this modified form of Eq. (40) is dubbed the *rigged* ETH.

Our findings exemplify that the ETH not only ensures thermalization at long times, but that it also has an impact on the full time-dependent relaxation process prior to equilibration. Moreover, we confirm our derivations by numerical results for idealized models of random-matrix type and more realistic models of interacting spins on a lattice.

Ref. [R8] *"Relaxation of dynamically prepared out-of-equilibrium initial states within and beyond linear response theory"*

In Refs. [R2], [R3], and [R6], we have studied the out-of-equilibrium dynamics resulting from the initial state $\rho(0)$ given in Eq. (61). In Ref. [R8], a slightly different nonequilibrium protocol is considered, where a quantum system at time $t=0$ is in thermal equilibrium,

$$\rho(0)=\rho_{\mathrm{eq}}=\frac{e^{-\beta\mathcal{H}_0}}{\mathrm{Tr}[e^{-\beta\mathcal{H}_0}]}\,, \tag{68}$$

and is suddenly subjected to an external force, which acts for times $0<t<t^*$. (Note that for small external forces, i.e., in the linear response regime, this nonequilibrium protocol can be related to the preparation scheme discussed in [R2, R3, R6].) Thus, the full (time-dependent) Hamiltonian $\mathcal{H}_t$ of the nonequilibrium protocol takes on the form

$$\mathcal{H}_t=\begin{cases}\mathcal{H}_0-\alpha\mathcal{O}\,, & 0<t<t^*\\ \mathcal{H}_0\,, & t>t^*\end{cases}\,, \tag{69}$$

and the initial equilibrium state $\rho(0)$ evolves for $t>0$ according to

$$\rho(t)=\begin{cases}e^{-i(\mathcal{H}_0-\alpha\mathcal{O})t}\rho(0)e^{i(\mathcal{H}_0-\alpha\mathcal{O})t}\,, & t<t^*\\ e^{-i\mathcal{H}_0(t-t^*)}\rho(t^*)e^{i\mathcal{H}_0(t-t^*)}\,, & t>t^*\end{cases}\,. \tag{70}$$

Due to the external force, the system is driven out of equilibrium and the expectation value $\langle\mathcal{O}(t)\rangle$ acquires a dependence on time. Upon switching off the force at $t=t^*$, $\langle\mathcal{O}(t)\rangle$ eventually equilibrates towards some constant long-time value $\mathcal{O}^\infty=\langle\mathcal{O}(t\to\infty)\rangle$.

In Ref. [R8], we find that this long-time value $\mathcal{O}^\infty$ exhibits an intriguing dependence on the strength of the external force for systems which violate the eigenstate thermalization hypothesis. Namely, for small external forces within the validity regime of LRT, the system relaxes back to its original equilibrium value, despite the ETH being violated. In contrast, for stronger perturbations beyond linear response, the quantum system relaxes to some nonthermal value which depends on the previous nonequilibrium protocol.

These results exemplify that (apart from the LRT regime) the ETH is indeed a physically necessary condition for initial-state-independent relaxation and thermalization in realistic situations. In particular, we numerically demonstrate our findings by studying the real-time dynamics of two ETH-violating quantum spin models.

Ref. [R7]: *"Dynamical typicality for initial states with a preset measurement statistics of several commuting observables"*

In contrast to the specific nonequilibrium situations studied in Refs. [R2, R3, R6, R8], Ref. [R7] considers the question of thermalization from a more abstract point of view and discusses an extension of the original dynamical typicality scenario from Ref. [85]. Namely, we consider a class of out-of-equilibrium initial states $\rho(0)$, for which the measurement outcomes of several commuting observables exhibit certain preset expectation values,

$$p_n=\mathrm{Tr}[\rho(0)P_n]\,. \tag{71}$$

Here, the P_n $(n=1,\ldots,N)$ denote the projectors onto the N common eigenspaces of the commuting observables with $\sum_{n=1}^N p_n=1$. A simple example for a set of mutually commuting operators is given by, e.g., the L local occupation number operators n_l [cf. Eq. (8)], where p_n can be adjusted between 0 and 1. Note that the knowledge of the full measurement statistics, i.e., fixing the values of the p_n, is still far from being sufficient to uniquely determine the actual microscopic initial state $\rho(0)$ of the system.

As a main result, it is shown in Ref. [R7] that the expectation-value dynamics $\mathrm{Tr}[A\rho(t)]$ of a given observable A and a single initial state $\rho(0)$ is practically indistinguishable from the ensemble-averaged dynamics over all $\rho(0)$ fulfilling Eq. (71). This result helps to better understand the well established fact that a few macroscopic features are sufficient to ensure the reproducibility of experimental measurements despite

many unknown and uncontrollable microscopic details of the system.

As an aside, Ref. [R7] also contains an introduction to the numerical aspects of dynamical quantum typicality, similar to the presentation in Sec. II.D. In this context, the smallness of the statistical error ϵ within the typicality approximation [cf. Eq. (42)] is demonstrated for the specific case with a preset measurement statistics of several commuting observables.

C. Development of numerical and (semi-)analytical approaches [R4, R10]

In Sec. II.D, dynamical quantum typicality and numerical linked cluster expansions have been introduced as two efficient methods to tackle the dynamics of quantum many-body systems. In Refs. [R4] and [R10], we show that DQT and NLCE can in fact be combined with each other. In particular, it is demonstrated that this combination yields a powerful approach to evaluate time-dependent correlation functions (i) in the thermodynamic limit $L \to \infty$ and (ii) for time scales similar or even longer compared to other state-of-the-art numerical methods. In Refs. [R4] and [R10], the combination of DQT and NLCE is particularly employed to study the spin-current autocorrelation function $\langle j(t)j\rangle_{\rm eq}$ in chain and ladder geometries.

As a central result, we show in Ref. [R4] that the time-dependent diffusion coefficient $D(t)$ [cf. Eq. (18)] in the isotropic and integrable Heisenberg chain diverges as a power-law at long times, $D(t) \propto t^{1/3}$. This finding indicates that, in contrast to the nonintegrable models considered in Sec. III.A, spin transport is not diffusive but superdiffusive instead. Moreover, the power-law divergence with the specific exponent $1/3$ numerically confirms a recent prediction [65], and is consistent with other studies which report that spin transport in this model is described by the Kardar-Parisi-Zhang universality class [107].

The determination of $\langle j(t)j\rangle_{\rm eq}$ by means of DQT and NLCE without finite-size effects plays an important role also in Ref. [R10]. Here, the decay of the current autocorrelation function is studied in nonintegrable ladder models, where the interchain couplings of the ladder are formally treated as a perturbation to the otherwise uncoupled legs. In this context, the precise knowledge of $\langle j(t)j\rangle_{\rm eq}$ in the unperturbed system (i.e. in chains) is crucial to perform perturbation theory (PT).

As a main result, we show in Ref. [R10] that for small to quite strong values of the interchain coupling, the exact dynamics of $\langle j(t)j\rangle_{\rm eq}$ in ladders agrees very well with the prediction from lowest-order PT. For small perturbations, for instance, the decay of $\langle j(t)j\rangle_{\rm eq}$ is essentially given by an exponential damping of the dynamics in the bare chains.

Ref. [R4]: *"Combining dynamical quantum typicality and numerical linked cluster expansions"*

As outlined in Sec. II.D, numerical linked cluster expansions provide a means to study quantum many-body systems directly in the thermodynamic limit. However, due to numerical limitations, the full sum in Eq. (48) has to be truncated to a maximum cluster size $c_{\rm max}$, which eventually results in a breakdown of convergence (beyond a certain time). In [R4], we demonstrate that $c_{\rm max}$ can be significantly increased thanks to a combination of NLCE with dynamical quantum typicality. Specifically, while the contributions of small clusters can still be obtained from diagonalization, larger clusters beyond the range of ED can be evaluated by DQT.

As a proof of principle, Ref. [R4] studies the dynamics of the current autocorrelation function $\langle j(t)j\rangle_{\rm eq}$ in the one-dimensional XXZ model. Importantly, it is demonstrated that for such a one-dimensional geometry, the identification of connected clusters becomes easy and the NLCE simplifies significantly. In fact, one can show that Eq. (48) reduces to

$$\langle j(t)j\rangle_{\rm eq}/L = \langle j(t)j\rangle_{\rm eq}^{(c_{\rm max})} - \langle j(t)j\rangle_{\rm eq}^{(c_{\rm max}-1)} \ , \quad (72)$$

which is just the difference between the two largest clusters. Despite its apparent simplicity, we unveil that Eq. (72) yields a convergence towards the thermodynamic limit already for small cluster sizes, which is substantially faster than in direct calculations of the autocorrelation function for systems with open or periodic boundary conditions.

While the focus of Ref. [R4] is on the isotropic Heisenberg chain at high temperatures (see discussion of superdiffusion above), Ref. [R4] also considers other anisotropies $\Delta \neq 1$, an integrability-breaking next-nearest neighbor interaction, and lower temperatures. While NLCE appears to work equally well for all parameter regimes, its advantage compared to standard ED or DQT is most pronounced for integrable models where finite-size effects are usually larger.

Ref. [R10]: *"Exponential damping induced by random and realistic perturbations"*

In Ref. [R10] we consider a quantum many-body system $\mathcal{H}_0$, which is affected by a perturbation $\mathcal{V}$, such that the total Hamiltonian takes on the form

$$\mathcal{H} = \mathcal{H}_0 + \lambda\mathcal{V} \ , \quad (73)$$

where λ denotes the strength of the perturbation. Moreover, $\langle\mathcal{O}(t)\rangle_{\mathcal{H}_0} = {\rm Tr}[\mathcal{O}e^{-i\mathcal{H}_0 t}\rho(0)e^{i\mathcal{H}_0 t}]$ denotes the expectation-value dynamics of some operator $\mathcal{O}$ with respect to the unperturbed system $\mathcal{H}_0$, where $\rho(0)$ is some out-of-equilibrium initial state. It is the main motivation of [R10] to answer the question, how this reference dynamics is altered due to the presence

of the perturbation $\mathcal{V}$, i.e., when $\rho(t)$ evolves with respect to the full Hamiltonian $\mathcal{H}$ instead of $\mathcal{H}_0$.

In Ref. [R10], we tackle this question by means of the time-convolutionless (TCL) projection-operator method [18]. While such projection-operator techniques are well-established in the context of open quantum systems, they can be applied to the dynamics of isolated systems as well, see, e.g., Ref. [108]. Omitting in this guide the technical details (on the choice of projectors and initial conditions), we restrict ourselves to the lowest nonvanishing order in perturbation theory, where the central object is the "damping rate"

$$\gamma_2(t) = \int_0^t \mathrm{d}t' \frac{\mathrm{Tr}\{i[\mathcal{O},\mathcal{V}_I(t')]i[\mathcal{O},\mathcal{V}]\}}{\mathrm{Tr}\{\mathcal{O}^2\}} \ . \tag{74}$$

Note that the subscript I indicates that the time evolution of $\mathcal{V}_I$ has to be understood with respect to the unperturbed system $\mathcal{H}_0$.

First, an idealized situation is considered where the Hamiltonian $\mathcal{H}_0$ has a high and almost uniform density of states, and the perturbation $\mathcal{V}$ is essentially a random matrix in the eigenbasis of $\mathcal{H}_0$. For this situation, we show that the unperturbed dynamics is exponentially damped according to

$$\langle \mathcal{O}(t) \rangle = \langle \mathcal{O}(t) \rangle_{\mathcal{H}_0} e^{-\lambda^2 \gamma t} \ , \tag{75}$$

where the value of γ can be obtained analytically starting from the expression given in Eq. (74) and agrees with Fermi's golden rule.

In order to test whether these findings for random perturbations are also relevant to realistic quantum many-body system, we moreover study the decay of the current autocorrelation function $C(t) = \langle j(t) j \rangle_{\mathrm{eq}}$ in spin-1/2 ladder systems, where the rungs of the ladder are treated as a perturbation to the otherwise uncoupled legs. While the exact dynamics in chains and ladders is obtained from the combination of NLCE and DQT, the second-order prediction from the TCL formalism reads

$$C(t) = C_0(t) \exp\left[-J_\perp^2 \int_0^t \mathrm{d}t' \gamma_2(t') \right] \ , \tag{76}$$

where $C_0(t)$ is the unperturbed dynamics in chains (see [R4]). Moreover, the damping rate $\gamma_2(t)$ can be evaluated by means of DQT for large systems. We find that Eq. (76) agrees very well with the exact dynamics for a wide range of interchain couplings $J_\perp$. This confirms that the analytical derivations in the context of Eq. (75) for ideal random matrices are also relevant to realistic perturbations and quantum many-body systems.

IV. CONCLUSION

Summary and discussion

Based on the works [R1] - [R10], various aspects of the dynamics of quantum many-body systems have been addressed in this dissertation. Particular emphasis has been given to the understanding of transport and thermalization phenomena in isolated (quasi) one-dimensional quantum spin systems.

As a first line of research, Refs. [R1], [R5], and [R9] have studied the transport properties for a variety of nonintegrable models within the framework of linear response theory. As a main result, the emergence of genuine diffusive transport has been detected for all integrability-breaking perturbations considered, i.e., next-nearest neighbor interactions, couplings between separate chains, and a higher spin quantum number $S = 1$. While it might not be entirely surprising that generic nonintegrable models exhibit diffusive transport at high temperatures, let us emphasize that the qualitative characterization of transport properties and the quantitative extraction of transport coefficients for microscopic models is a challenge to theory. In this context, we have demonstrated that dynamical quantum typicality provides an efficient method to obtain time-dependent equilibrium correlation functions for large systems and long time scales.

As a second line of research, Refs. [R2], [R3], [R6], [R7], and [R8] have scrutinized the time-dependent relaxation process of quantum expectation values in different out-of-equilibrium situations. First, in Refs. [R2], [R3], and [R6], we have considered a realistic class of initial states, which are thermal states of the model in the presence of an additional static force, but become nonequilibrium states after a sudden removal of this force. Remarkably, it has been found that for high temperatures and specific classes of operators, the resulting relaxation process can become independent of whether the initial state is prepared close to or far away from equilibrium. Furthermore, in Ref. [R8], a different but related quench protocol has been studied, where out-of-equilibrium conditions are dynamically generated due to an explicit time-dependence of the Hamiltonian. Here, we have exemplified that the ETH is indeed a physically necessary condition for initial-state-independent relaxation and thermalization in realistic situations.

Finally, in Refs. [R4] and [R10], a combination of dynamical quantum typicality and numerical linked cluster expansions has been introduced as a powerful approach to study quantum many-body dynamics in the thermodynamic limit for comparatively long time scales. We have employed this numerical tool to study current autocorrelation functions in chain and ladder geometries. In this context, we have shown that high-temperature spin transport in the integrable and isotropic Heisenberg chain is superdiffusive with a di-

verging diffusion coefficient $D(t) \propto t^{1/3}$. Furthermore, we have demonstrated that for small to quite strong interchain couplings, the decay of currents in ladders can be understood within lowest-order perturbation theory as an exponential damping of the original dynamics in chains. Based on analytical calculations for idealized random-matrix models, we have argued that the phenomenon of an exponential damping can appear in many perturbed quantum many-body systems (see also Ref. [109]).

Outlook

While this thesis has already studied various questions within the vast field of quantum many-body dynamics, some topics have naturally remained untouched. Therefore, based on the results of this dissertation, let us briefly outline some promising directions of future research.

From a numerical point of view, a first obvious step would be to apply the combination of DQT and NLCE to questions on transport and thermalization in other (more complicated) models beyond the ones studied in this thesis. For instance, while we have so far considered short-ranged models comprising nearest and next-nearest neighbor terms only, models with power-law interactions (i.e. with couplings decaying as $J_{ll'} \propto 1/|l - l'|^{\alpha}$) are relevant to describe the physics of atomic or molecular systems, where dipolar or van der Waals interactions can be present [110]. In addition, it would be interesting to extend the combination of DQT and NLCE also to two-dimensional lattices, where fewer numerical methods are available to reliably simulate quantum many-body dynamics in real time.

From a conceptual point of view, parts of our analytical results presented in Refs. [R6] and [R10] relied on the assumption that physical operators in the eigenbasis of the underlying Hamiltonian can be described in terms of random matrices, similar to the ETH ansatz (40). While we have numerically demonstrated that this assumption can in some cases hold to very good quality, it is certainly questionable that a unitary basis transformation of a nonrandom operator yields entirely uncorrelated matrix elements. In fact, it has been argued that correlations between matrix elements are essential to explain the growth of certain four-point correlation functions (so-called out-of-time-ordered correlators) [111]. Identifying the pertinent correlations between matrix elements and understanding their implications on our results in Refs. [R6] and [R10] promises to be an interesting avenue of future research.

REFERENCES

[R1] J. Richter, F. Jin, H. De Raedt, K. Michielsen, J. Gemmer, and R. Steinigeweg, Phys. Rev. B **97**, 174430 (2018).
[R2] J. Richter, J. Herbrych, and R. Steinigeweg, Phys. Rev. B **98**, 134302 (2018).
[R3] J. Richter and R. Steinigeweg, Phys. Rev. E **99**, 012114 (2019).
[R4] J. Richter and R. Steinigeweg, Phys. Rev. B **99**, 094419 (2019).
[R5] J. Richter, F. Jin, L. Knipschild, J. Herbrych, H. De Raedt, K. Michielsen, J. Gemmer, and R. Steinigeweg, Phys. Rev. B **99**, 144422 (2019).
[R6] J. Richter, J. Gemmer, and R. Steinigeweg, Phys. Rev. E **99**, 050104(R) (2019).
[R7] B. N. Balz, J. Richter, J. Gemmer, R. Steinigeweg, and P. Reimann, in *Thermodynamics in the Quantum Regime. Fundamental Aspects and New Directions* (Springer, Cham, 2019).
[R8] J. Richter, M. H. Lamann, C. Bartsch, R. Steinigeweg, and J. Gemmer, Phys. Rev. E **100**, 032124 (2019).
[R9] J. Richter, N. Casper, W. Brenig, R. Steinigeweg, Phys. Rev B **100**, 144423 (2019).
[R10] J. Richter, F. Jin, L. Knipschild, H. De Raedt, K. Michielsen, J. Gemmer, and R. Steinigeweg, arXiv:1906.09268.
[R11] J. Richter, D. Schubert, and R. Steinigeweg, arXiv:1911.09917.
[12] C. Gogolin and J. Eisert, Rep. Prog. Phys. **79**, 056001 (2016).
[13] L. D'Alessio, Y. Kafri, A. Polkovnikov, and M. Rigol, Adv. Phys. **65**, 239 (2016).
[14] W. Brenig, *Statistische Theorie der Wärme. Gleichgewichtsphänomene* (Springer, Berlin, 1996).
[15] J. L. Lebowitz and O. Penrose, Physics Today **26**, 23 (1973).
[16] J. L. Lebowitz, Physics Today **46**, 32 (1993).
[17] F. Borgonovi, F. M. Izrailev, L. F. Santos, and V. G. Zelevinsky, Phys. Rep. **626**, 1 (2016).
[18] H.-P. Breuer and F. Petruccione, *The Theory of Open Quantum Systems* (Oxford University Press, New York, 2007).
[19] A. Polkovnikov, K. Sengupta, A. Silva, and M. Vengalattore, Rev. Mod. Phys. **83**, 863 (2011).
[20] J. Eisert, M. Friesdorf, and C. Gogolin, Nat. Phys. **11**, 124 (2015).
[21] I. Bloch, J. Dalibard, and S. Nascimbène, Nat. Phys. **8**, 267 (2012).
[22] R. Blatt and C. F. Roos, Nat. Phys. **8**, 277 (2012).
[23] J. von Neumann, Z. Phys. **57**, 30 (1929).
[24] S. Lloyd, Ph.D. Thesis, The Rockefeller University (1988), Chapter 3, arXiv:1307.0378.
[25] J. Gemmer, M. Michel, and G. Mahler, *Quantum Thermodynamics* (Springer, Berlin, 2004).
[26] S. Popescu, A. J. Short, and A. Winter, Nat. Phys. **2**, 754 (2006).
[27] S. Goldstein, J. L. Lebowitz, R. Tumulka, and N. Zanghì, Phys. Rev. Lett. **96**, 050403 (2006).
[28] P. Reimann, Phys. Rev. Lett. **99**, 160404 (2007).
[29] J. M. Deutsch, Phys. Rev. A **43**, 2046 (1991).
[30] M. Srednicki, Phys. Rev. E **50**, 888 (1994).
[31] M. Rigol, V. Dunjko, and M. Olshanii, Nature **452**, 854 (2008).
[32] U. Schollwöck, Ann. Phys. **326**, 96 (2011).

[33] A. Mitra, Annu. Rev. Condens. Matter Phys. **9**, 245 (2018).
[34] P. Reimann, Nat. Commun. **7**, 10821 (2016).
[35] R. Kubo, M. Toda, and N. Hashitsume, *Statistical Physics II: Nonequilibrium Statistical Mechanics*, Solid-State Sciences **31** (Springer, Berlin, 1991).
[36] M. Buchanan, Nat. Phys. **1**, 71 (2005).
[37] A. Auerbach, *Interacting Electrons and Quantum Magnetism* (Springer, New York, 1994).
[38] P. Jordan and E. Wigner, Z. Phys. **47**, 631 (1928).
[39] M. A. Cazalilla, R. Citro, T. Giamarchi, E. Orignac, and M. Rigol, Rev. Mod. Phys. **83**, 1405 (2011).
[40] D. C. Johnston, R. K. Kremer, M. Troyer, X. Wang, A. Klümper, S. L. Bud'ko, A. F. Panchula, and P. C. Canfield, Phys. Rev. B **61**, 9558 (2000).
[41] H.-J. Mikeska and A. K. Kolezhuk, Lect. Notes Phys. **645**, 1 (2004).
[42] V. I. Arnold, *Mathematical Methods of Classical Mechanics* (Springer, New York, 1978).
[43] J.-S. Caux and J. Mossel, J. Stat. Mech. **(2011)**, 02023 (2011).
[44] H. Bethe, Z. Phys. **71**, 205 (1931).
[45] V. E. Korepin, N. M. Bogoliubov, and A. G. Izergin, *Quantum Inverse Scattering Method and Correlation Functions* (Cambridge University Press, Cambridge, 1993).
[46] T. A. Brody, J. Flores, J. B. French, P. A. Mello, A. Pandey, and S. S. M. Wong, Rev. Mod. Phys. **53**, 385 (1981).
[47] M. V. Berry and M. Tabor, Proc. R. Soc. Lond. A **356**, 375 (1977).
[48] O. Bohigas, M. J. Giannoni, and C. Schmit, Phys. Rev. Lett. **52**, 1 (1984).
[49] L. F. Santos and M. Rigol, Phys. Rev. E **82**, 031130 (2010).
[50] D. J. Luitz and Y. Bar Lev, Phys. Rev. Lett. **117**, 170404 (2016).
[51] S. A. Wolf, D. D. Awschalom, R. A. Buhrman, J. M. Daughton, S. von Molnár, M. L. Roukes, A. Y. Chtchelkanova, and D. Treger, Science **294**, 1488 (2001).
[52] F. Heidrich-Meisner, A. Honecker, and W. Brenig, Eur. Phys. J. Spec. Top. **151**, 135 (2007).
[53] R. Steinigeweg and J. Gemmer, Phys. Rev. B **80**, 184402 (2009).
[54] K. Fabricius, U. Löw, and J. Stolze, Phys. Rev. B **55**, 5833 (1997).
[55] B. Lake, D. A. Tennant, J.-S. Caux, T. Barthel, U. Schollwöck, S. E. Nagler, and C. D. Frost, Phys. Rev. Lett. **111**, 137205 (2013).
[56] P. Mazur, Physica (Amsterdam) **43**, 533 (1969).
[57] X. Zotos, F. Naef, and P. Prelovšek, Phys. Rev. B **55**, 11029 (1997).
[58] T. Prosen, Phys. Rev. Lett. **106**, 217206 (2011).
[59] T. Prosen and E. Ilievski, Phys. Rev. Lett. **111**, 057203 (2013).
[60] F. Heidrich-Meisner, A. Honecker, D. C. Cabra, and W. Brenig, Phys. Rev. B **68**, 134436 (2003).
[61] M. Žnidarič, Phys. Rev. Lett. **106**, 220601 (2011).
[62] R. Steinigeweg and W. Brenig, Phys. Rev. Lett. **107**, 250602 (2011).
[63] C. Karrasch, J. E. Moore, and F. Heidrich-Meisner, Phys. Rev. B **89**, 075139 (2014).
[64] M. Ljubotina, M. Žnidarič, and T. Prosen, Nat. Comm. **8**, 16117 (2017).
[65] S. Gopalakrishnan and R. Vasseur, Phys. Rev. Lett. **122**, 127202 (2019).
[66] M. Srednicki, J. Phys. A **32**, 1163 (1999).
[67] R. Steinigeweg, J. Herbrych, and P. Prelovšek, Phys. Rev. E **87**, 012118 (2013).
[68] W. Beugeling, R. Moessner, and M. Haque, Phys. Rev. E **89**, 042112 (2014).
[69] H. Kim, T. N. Ikeda, D. A. Huse, Phys. Rev. E **90**, 052105 (2014).
[70] R. Mondaini and M. Rigol, Phys. Rev. E **96**, 012157 (2017).
[71] M. Rigol, V. Dunjko, V. Yurovsky, and M. Olshanii, Phys. Rev. Lett. **98**, 050405 (2007).
[72] E. T. Jaynes, Phys. Rev. **106**, 620 (1957); **108**, 171 (1957).
[73] D. M. Basko, I. L. Aleiner, and B. L. Altshuler, Ann. Phys. **321**, 1126 (2006).
[74] R. Nandkishore and D. A. Huse, Annu. Rev. Condens. Matter Phys. **6**, 15 (2015).
[75] D. A. Abanin, E. Altman, I. Bloch, and M. Serbyn, Rev. Mod. Phys. **91**, 021001 (2019).
[76] M. Serbyn, Z. Papić, and D. A. Abanin, Phys. Rev. Lett. **111**, 127201 (2013).
[77] D. A. Huse, R. Nandkishore, and V. Oganesyan, Phys. Rev. B **90**, 174202 (2014).
[78] A. Pal and D. A. Huse, Phys. Rev. B **82**, 174411 (2010).
[79] E. Gull, A. J. Millis, A. I. Lichtenstein, A. N. Rubtsov, M. Troyer, and P. Werner, Rev. Mod. Phys. **83**, 349 (2011).
[80] H. Aoki, N. Tsuji, M. Eckstein, M. Kollar, T. Oka, and P. Werner, Rev. Mod. Phys. **86**, 779 (2014).
[81] M. W. Long, P. Prelovšek, S. El Shawish, J. Karadamoglou, and X. Zotos, Phys. Rev. B **68**, 235106 (2003).
[82] G. Carleo and M. Troyer, Science **355**, 602 (2017).
[83] G. Vidal, Phys. Rev. Lett. **93**, 040502 (2004).
[84] A. W. Sandvik, AIP Conference Proceedings **1297**, 135 (2010).
[85] C. Bartsch and J. Gemmer, Phys. Rev. Lett. **102**, 110403 (2009).
[86] T. Iitaka and T. Ebisuzaki, Phys. Rev. Lett. **90**, 047203 (2003).
[87] T. A. Elsayed and B. V. Fine, Phys. Rev. Lett. **110**, 070404 (2013).
[88] R. Steinigeweg, J. Gemmer, and W. Brenig, Phys. Rev. Lett. **112**, 120601 (2014).
[89] A. Hams and H. De Raedt, Phys. Rev. E **62**, 4365 (2000).
[90] S. Sugiura and A. Shimizu, Phys. Rev. Lett. **111**, 010401 (2013).
[91] H. De Raedt and K. Michielsen, in *Handbook of Theoretical and Computational Nanotechnology* (American Scientific Publishers, Los Angeles, 2006).
[92] V. V. Dobrovitski and H. De Raedt, Phys. Rev. E **67**, 056702 (2003).
[93] A. Weiße, G. Wellein, A. Alvermann, and H. Fehske, Rev. Mod. Phys. **78**, 275 (2006).
[94] A. Nauts and R. E. Wyatt, Phys. Rev. Lett. **51**, 2238 (1983).
[95] M. Rigol, T. Bryant, and R. R. P. Singh, Phys. Rev. Lett. **97**, 187202 (2006).
[96] B. Tang, E. Khatami, and M. Rigol, Comput. Phys. Commun. **184**, 557 (2013).
[97] K. Mallayya and M. Rigol, Phys. Rev. Lett. **120**, 070603 (2018).
[98] J. Oitmaa, C. Hamer, and W. Zheng, *Series Expan-*

sion Methods for Strongly Interacting Lattice Models (Cambridge University Press, Cambridge, 2006).
[99] H. Castella, X. Zotos, and P. Prelovšek, Phys. Rev. Lett. **74**, 972 (1995).
[100] M. Brenes, E. Mascarenhas, M. Rigol, and J. Goold, Phys. Rev. B **98**, 235128 (2018).
[101] R. Steinigeweg, F. Jin, D. Schmidtke, H. de Raedt, K. Michielsen, and J. Gemmer, Phys. Rev. B **95**, 035155 (2017).
[102] D. N. Page, Phys. Rev. Lett. **71**, 1291 (1993).
[103] L. Knipschild and J. Gemmer, Phys. Rev. E **98**, 062103 (2018).
[104] J. De Nardis, M. Medenjak, C. Karrasch, and E. Ilievski, Phys. Rev. Lett. **123**, 186601 (2019).
[105] M. Dupont and J. E. Moore, arXiv:1907.12115.
[106] D. J. Luitz and Y. Bar Lev, Ann. Phys. **529**, 1600350 (2017).
[107] M. Ljubotina, M. Žnidarič, and T. Prosen, Phys. Rev. Lett. **122**, 210602 (2019).
[108] R. Steinigeweg, J. Gemmer, H.-P. Breuer, and H.-J. Schmidt, Eur. Phys. J. B **69**, 275 (2009).
[109] L. Dabelow and P. Reimann, arXiv:1903.11881.
[110] M. Saffman, T. G. Walker, and K. Mølmer, Rev. Mod. Phys. **82**, 2313 (2010).
[111] L. Foini and J. Kurchan, Phys. Rev. E **99**, 042139 (2019).

Acknowledgements

It is my pleasure to acknowledge support from the many persons who have impacted the outcome of this thesis. First of all, I am truly grateful to Robin Steinigeweg. You have been the ideal mentor since my undergraduate studies in Braunschweig, and I want to thank you very much for giving me the opportunity to join your "one-man group" in Osnabrück. During the last three years, you have taught me to write beautiful scientific papers and how to navigate through the academic world. Thank you for always finding the time when I needed some feedback or some brainstorming, for your constant interest in the progress of my work, and for the possibility to visit many conferences and schools.

I would also like to express my gratitude to my "PhD grandfather" Jochen Gemmer. Your profound knowledge of different aspects of physics has been invaluable for the success of many publications, and I think that I have learned a lot from each discussion we had. Moreover, your thoughts on science and on the world in general have made the daily coffee breaks quite stimulative and entertaining.

This cumulative dissertation would have been impossible without my (other) coauthors and colleagues. In particular, collaborations with the "Jülich gang" including Fengping Jin, Hans de Raedt, and Kristel Michielsen have always been very pleasant and productive. Moreover, I am thankful to Jacek Herbrych, not only for our collaborations, but also for the fun times we had in Los Angeles and Boston. Many thanks go to the colleagues in Bielefeld, especially Ben Balz, Christian Bartsch, and Peter Reimann. Furthermore, I thank my former adviser Wolfram Brenig who supported my decision to take the step from Braunschweig to Osnabrück. I also thank the other PhD students from the theory groups in Osnabrück, namely, Lars Knipschild (who was there from the very beginning), Tjark Heitmann, Robin Heveling, and Dennis Schubert (who all joined a little later), as well as Mats Lamann. A special thanks goes to Christoph Schiel and Dominik Lips for our great Chinatown experience in Boston. Last but not least, I am thankful to my good friend Niklas Casper. I am glad that we have managed to work on a paper together, and I wish you all the best for your own PhD.

I am indebted to my parents for supporting me throughout my studies, as well as for providing guidance and stability whenever I needed some advice. Thank you that I always could (and still always can) rely on you! Furthermore, I thank my brother Jan whom I wish all the best on his way to become a fantastic physicist.

Finally, I am deeply thankful to Jana for being by my side, for being understanding even when my mind was occupied with physics after hours and, at the same time, for reminding me that there is a world outside of physics.

Preprint of Ref. [R10]

Jonas Richter, Fengping Jin, Lars Knipschild, Hans De Raedt, Kristel Michielsen, Jochen Gemmer, and Robin Steinigeweg,

"Exponential damping induced by random and realistic perturbations".

`https://arxiv.org/abs/1906.09268`

Exponential damping induced by random and realistic perturbations

Jonas Richter,[1,*] Fengping Jin,[2] Lars Knipschild,[1] Hans De Raedt,[3]
Kristel Michielsen,[2,4] Jochen Gemmer,[1,†] and Robin Steinigeweg[1,‡]

[1] *Department of Physics, University of Osnabrück, D-49069 Osnabrück, Germany*
[2] *Institute for Advanced Simulation, Jülich Supercomputing Centre, Forschungszentrum Jülich, D-52425 Jülich, Germany*
[3] *Zernike Institute for Advanced Materials, University of Groningen, NL-9747AG Groningen, The Netherlands*
[4] *RWTH Aachen University, D-52056 Aachen, Germany*

(Dated: June 25, 2019)

Given a quantum many-body system and the expectation-value dynamics of some operator, we study how this reference dynamics is altered due to a perturbation of the system's Hamiltonian. Based on projection operator techniques, we unveil that if the perturbation exhibits a random-matrix structure in the eigenbasis of the unperturbed Hamiltonian, then this perturbation effectively leads to an exponential damping of the original dynamics. Employing a combination of dynamical quantum typicality and numerical linked cluster expansions, we demonstrate that our theoretical findings are relevant for the dynamics of realistic quantum many-body models. Specifically, we study the decay of current autocorrelation functions in spin-1/2 ladder systems, where the rungs of the ladder are treated as a perturbation to the otherwise uncoupled legs. We find a convincing agreement between the exact dynamics and the lowest-order prediction over a wide range of interchain couplings, even if the perturbation is not weak.

Introduction. Understanding the dynamics of interacting quantum many-body systems is notoriously challenging. While their complexity grows exponentially in the number of degrees of freedom, the strong correlations between the constituents often prohibit any exact solution. Although much progress has been made due to the development of powerful numerical machinery [1] and the advance of controlled experimental platforms [2, 3], the detection of general (i.e. universal) principles which underlie the emerging many-body dynamics is of fundamental importance [4]. To this end, a remarkably successful strategy in the past has been the usage of random-matrix ensembles instead of treating the full many-body problem. Ranging back to the description of nuclei spectra [5] and of quantum chaos in systems with classical counterparts [6], random-matrix theory also forms the backbone of the celebrated eigenstate thermalization hypothesis [7–9], which provides a microscopic explanation for the emergence of thermodynamic behavior in isolated quantum systems. More recently, random-circuit models have led to new insights into the scrambling of information and the onset of hydrodynamic transport in quantum systems undergoing unitary time evolution [10–12].

Concerning the out-of-equilibrium dynamics of quantum many-body systems, a particularly intriguing question is how the expectation-value dynamics of some operator is altered if the system's Hamiltonian is modified by a (small) perturbation. Clearly, the effect of such a perturbation in a (integrable or chaotic) system can be manifold. In the context of prethermalization [13–18], the perturbation breaks a conservation law of the (usually integrable) reference Hamiltonian, leading to a separation of time scales, where the system stays close to some long-lived nonthermal state, before eventually giving in to its thermal fate at much longer times. Moreover, in the study of echo protocols, time-local perturbations have been shown to entail irreversible quantum dynamics [19], analogous to the butterfly effect in classical chaotic systems. Furthermore, the observation that some types of temporal relaxation, such as the exponential decay, are more common than others can be traced back to their enhanced stability against perturbations [20].

In this Letter, we build upon the success of random-matrix models and consider perturbations with a random matrix structure in the eigenbasis of the unperturbed Hamiltonian. Based on projection operator techniques, we unveil that, in such a case, the perturbation effectively leads to an exponential damping of the original expectation-value dynamics, similar to recent results in Ref. [21] (see also the examples [22–25] discussed therein). Employing state-of-the-art numerics, we demonstrate that our theoretical findings are readily applicable to realistic quantum many-body models.

Projection-operator approach. We consider a closed quantum many-body system $\mathcal{H}_0$ which is affected by a perturbation $\mathcal{V}$, such that the total Hamiltonian reads $\mathcal{H} = \mathcal{H}_0 + \lambda\mathcal{V}$, where λ denotes the strength of the perturbation. Moreover, we study how the expectation-value dynamics of some operator, $\langle\mathcal{O}(t)\rangle = \mathrm{Tr}[\rho(t)\mathcal{O}]$, is altered due to the presence of the perturbation (compared to its bare dynamics under $\mathcal{H}_0$), where $\rho(t) = e^{-i\mathcal{H}t}\rho(0)e^{i\mathcal{H}t}$, and $\rho(0)$ is a (mixed or pure) initial state. We tackle this question by means of a projection-operator approach, i.e., the so-called time-convolutionless (TCL) method (see [26, 27] for a comprehensive overview).

In order to simplify the following derivations, let us assume that $\mathcal{H}_0$ has a very high and almost uniform density of states $\Omega \approx 1/\Delta\omega$, where $\Delta\omega$ is the mean

level spacing. Moreover, we shift the true eigenvalues of $\mathcal{H}_0$ slightly, such that they result as $E_\omega = \Delta\omega \cdot \omega$, with ω being an integer. For times $t \ll 2\pi/\Delta\omega$, the dynamics of this "shifted" $\mathcal{H}_0$ should be indistinguishable from the original one. Furthermore, we define a Fourier component of the operator $\mathcal{O}$ in the eigenbasis of $\mathcal{H}_0$, $\mathcal{O}_\omega = 1/\sqrt{z_\omega}\sum_\eta |\eta\rangle \mathcal{O}_{\eta,\eta+\omega} \langle \eta+\omega| + \text{h.c.}$, with normalization $z_\omega = 2\sum_\eta |\mathcal{O}_{\eta,\eta+\omega}|^2$, and construct a set of corresponding projection operators $\mathcal{P}_\omega$, which project onto the relevant part of the density matrix $\rho(t)$, $\mathcal{P}_\omega\rho(t) = \text{Tr}[\rho(t)\mathcal{O}_\omega]\mathcal{O}_\omega$. Note that, from the definition of $\mathcal{O}_\omega$, it immediately follows that $\langle\mathcal{O}(t)\rangle = \sum_\omega \sqrt{z_\omega}\langle\mathcal{O}_\omega(t)\rangle$, which holds for any $\mathcal{H}$, and in the special case $\lambda = 0$, we can further write $\langle\mathcal{O}(t)\rangle_{\mathcal{H}_0} = \sum_\omega \sqrt{z_\omega}\langle\mathcal{O}_\omega(0)\rangle \cos(\Delta\omega \cdot \omega t)$. In particular, the dynamics of $\mathcal{O}_\omega$ in the Schrödinger picture and in the interaction picture (subscript I) are related by $\text{Tr}[\mathcal{O}_\omega\rho(t)] = \text{Tr}[\mathcal{O}_\omega\rho_I(t)]\cos(\Delta\omega \cdot \omega t)$. Tacitly focusing on initial states with $\mathcal{P}_\omega\rho(0) = \rho(0)$ [28], the TCL framework then yields a time-local equation for $\mathcal{O}_{I,\omega}(t) \equiv \text{Tr}[\mathcal{O}_\omega\rho_I(t)]$, comprising a systematic perturbation expansion in powers of λ,

$$\dot{\mathcal{O}}_{I,\omega}(t) = -\gamma_\omega(t)\mathcal{O}_{I,\omega}(t) \; ; \quad \gamma_\omega(t) = \sum_n \lambda^n \gamma_{\omega,n}(t) \; , \quad (1)$$

where the $\gamma_{\omega,n}(t)$ are time-dependent rates of n-th order. Since the odd orders of this expansion vanish for many models, the leading-order term is $\gamma_{\omega,2}(t) = \int_0^t \mathrm{d}t' K_{\omega,2}(t') = \int_0^t \mathrm{d}t' \text{Tr}\{i[\mathcal{O}_\omega, \mathcal{V}_I(t')]i[\mathcal{O}_\omega, \mathcal{V}]\}$, where $\mathcal{V}_I(t) = e^{i\mathcal{H}_0 t}\mathcal{V}e^{-i\mathcal{H}_0 t}$, and the second-order kernel can be rewritten as $K_{\omega,2}(t) = \widetilde{K}_{\omega,2}(t) + \widehat{K}_{\omega,2}(t)$, with

$$\widetilde{K}_{\omega,2}(t) = \text{Tr}\left[-\mathcal{O}_\omega\mathcal{V}_I(t)\mathcal{O}_\omega\mathcal{V} - \mathcal{V}_I(t)\mathcal{O}_\omega\mathcal{V}\mathcal{O}_\omega\right] , \quad (2)$$

$$\widehat{K}_{\omega,2}(t) = \text{Tr}\left[\mathcal{O}_\omega\mathcal{V}_I(t)\mathcal{V}\mathcal{O}_\omega + \mathcal{O}_\omega\mathcal{V}\mathcal{V}_I(t)\mathcal{O}_\omega\right] . \quad (3)$$

Let us now assume that $\mathcal{V}$ essentially is a *random* (and possibly banded) matrix in the eigenbasis of the unperturbed system $\mathcal{H}_0$. In this case, the terms in (2) consist of sums in which each addend carries a product of two uncorrelated random numbers. If the random numbers have mean zero, these sums should be negligible, $\widetilde{K}_{\omega,2}(t) \approx 0$. In contrast, the terms in (3) do contribute, and we find

$$\begin{aligned}\widehat{K}_{\omega,2}(t) &= \frac{4}{z_\omega}\sum_{\eta,\kappa} |\mathcal{V}_{\kappa,\eta}|^2 |\mathcal{O}_{\eta,\eta+\omega}|^2 \cos\left[(\kappa-\eta)\Delta\omega t\right] \\ &\approx \frac{4\Omega\overline{v^2}}{z_\omega}\sum_\eta \int_{-W}^{W} |\mathcal{O}_{\eta,\eta+\omega}|^2 \cos(\chi t)\,\mathrm{d}\chi \qquad (4) \\ &= 2\Omega\overline{v^2}\int_{-W}^{W}\cos(\chi t)\,\mathrm{d}\chi = 4\Omega\overline{v^2}\,\frac{\sin(Wt)}{t} \; . \quad (5)\end{aligned}$$

Several comments are in order. Since $\mathcal{V}$ is a random matrix, we have approximated in Eq. (4) all squared individual matrix elements by their averages $\overline{v^2}$, i.e., $|\mathcal{V}_{\kappa,\eta}|^2 \approx \overline{v^2}$. Furthermore, we have used an index shift $\kappa \to \chi + \eta$ and converted the original sum over κ to an integral, where W denotes the half-bandwidth of $\mathcal{V}$. From (4) to (5), we have exploited that sum and integral can be evaluated independently and used the definition of z_ω. Inserting (5) into the definition of $\gamma_{\omega,2}(t)$ then yields $\gamma_{\omega,2}(t) \approx 4\Omega\overline{v^2}\int_0^t \mathrm{d}t' \sin(Wt')/t' \approx 2\pi\Omega\overline{v^2}$, for times $t \gg \pi/W$. Thus, $\gamma_{\omega,2}(t)$ is essentially a constant (Fermi's Golden Rule) rate, and we abbreviate $\gamma = 2\pi\Omega\overline{v^2}$. Moreover, it follows from Eq. (1) that $\mathcal{O}_{I,\omega}(t) = \langle\mathcal{O}_\omega(0)\rangle e^{-\lambda^2\gamma t}$. Transforming back into the Schrödinger picture and comparing the expressions for $\langle\mathcal{O}_\omega(t)\rangle$ and $\langle\mathcal{O}_\omega(t)\rangle_{\mathcal{H}_0}$ [above Eq. (1)], we find

$$\langle\mathcal{O}(t)\rangle = \langle\mathcal{O}(t)\rangle_{\mathcal{H}_0} e^{-\lambda^2\gamma t} \; . \quad (6)$$

This exponential damping of expectation-value dynamics induced by random perturbations is a central result of the present Letter, and consistent with recent results in Ref. [21]. While our derivations are rigorous up to second order in the perturbation strength [28], the evaluation of higher order corrections is a daunting task in practice [29] and, for random matrices, these corrections are expected to be irrelevant [30, 31]. Hence, apart from this truncation, the most crucial point is whether or not a random-matrix description is indeed justified for realistic physical perturbations (see also [32–34]). Therefore, let us exemplify that our findings are indeed applicable to generic quantum many-body systems.

Numerical Illustration. As an example, we study a (quasi-)one-dimensional spin-1/2 lattice model with ladder geometry [35–39], where the rung part of the ladder is treated as a perturbation to the otherwise uncoupled legs, i.e., the Hamiltonian reads $\mathcal{H} = J_\parallel\mathcal{H}_0 + J_\perp\mathcal{V}$, with

$$\mathcal{H}_0 = \sum_{l=1}^{L}\sum_{k=1}^{2}\mathbf{S}_{l,k}\cdot\mathbf{S}_{l+1,k} \; ; \quad \mathcal{V} = \sum_{l=1}^{L}\mathbf{S}_{l,1}\cdot\mathbf{S}_{l,2} \; . \quad (7)$$

Here, $\mathbf{S}_{l,k} = (S^x_{l,k}, S^y_{l,k}, S^z_{l,k})$ are spin-1/2 operators, $J_\parallel$ ($J_\perp$) is the coupling constant on the legs (rungs), and L denotes the length of the ladder. While, for $J_\perp = 0$, $\mathcal{H}$ consists of two separate Heisenberg chains and is integrable, this integrability is broken for any $J_\perp \neq 0$.

Let us study the current autocorrelation function $C(t) = \langle j(t)j\rangle_{\text{eq}}/L = \text{Tr}[\rho_{\text{eq}}j(t)j]/L$ [40], where $\rho_{\text{eq}} = e^{-\beta\mathcal{H}}/\mathcal{Z}$ is the canonical density matrix, $\beta = 1/T$ denotes the inverse temperature, and $j(t) = e^{i\mathcal{H}t}je^{-i\mathcal{H}t}$. The spin-current operator j follows from a lattice continuity equation [43], and is given by $j = J_\parallel\sum_l\sum_k(S^x_{l,k}S^y_{l+1,k} - S^y_{l,k}S^x_{l+1,k})$. Importantly, j is independent of the perturbation $\mathcal{V}$. The correlation function $C(t)$ is an important quantity in the context of transport. Despite the integrability of $\mathcal{H}_0$, the dynamics of $C(t)$ is nontrivial even for $J_\perp = 0$ [44]. While $C(t)$ has been numerically studied by various methods [38, 45, 46], we here rely on a powerful combination of dynamical quantum typicality (DQT) [47–57] and numerical linked cluster expansions (NLCE) [58, 59], recently put forward by two of us [60].

On the one hand, the concept of DQT relies on the fact that a single pure quantum state can imitate the full statistical ensemble. Specifically, $C(t)$ can be written as a scalar product with the two pure states $|\psi_\beta(t)\rangle = e^{-i\mathcal{H}t} j\,|\varphi_\beta\rangle$ and $|\varphi_\beta(t)\rangle = e^{-i\mathcal{H}t}\,|\varphi_\beta\rangle$, i.e., $C(t) = \langle\varphi_\beta(t)|\,j\,|\psi_\beta(t)\rangle\,/L\,\langle\varphi_\beta|\varphi_\beta\rangle + \epsilon$ [55, 56], where $|\varphi_\beta\rangle = e^{-\beta\mathcal{H}/2}\,|\varphi\rangle$, and $|\varphi\rangle$ is randomly drawn (Haar measure [51]) from the full Hilbert space with dimension $D = 4^L$. Importantly, the statistical error $\epsilon = \epsilon(|\varphi\rangle)$ vanishes as $\epsilon \propto 1/\sqrt{D}$ (for $\beta = 0$), and the typicality approximation becomes practically exact already for moderate values of L. Since the time evolution of pure states can be conveniently evaluated by iteratively solving the real-time Schrödinger equation, e.g., by means of fourth-order Runge-Kutta [55, 56] or a Trotter product formula [61], it is possible to treat large D, out of reach for standard exact diagonalization (ED).

On the other hand, NLCE provides a means to obtain $C(t)$ directly in the thermodynamic limit $L \to \infty$. Specifically, the current autocorrelation is calculated as the sum of contributions from all connected clusters which can be embedded on the lattice [58], $\langle j(t)j\rangle_{\rm eq}/L = \sum_c \mathcal{L}_c W_c(t)$, where $W_c(t)$ is the weight of cluster c with multiplicity $\mathcal{L}_c$. Moreover, the weights $W_c(t)$ are obtained by the so-called inclusion-exclusion principle, $W_c(t) = \langle j(t)j\rangle_{\rm eq}^{(c)} - \sum_{s\subset c} W_s(t)$, where $\langle j(t)j\rangle_{\rm eq}^{(c)}$ denotes the (extensive) current autocorrelation evaluated on the cluster c (with open boundary conditions), and the sum runs over all subclusters of c. In practice, this series has to be truncated to a maximum cluster size $c_{\rm max}$. This truncation in turn leads to a breakdown of convergence of $C(t)$ at some time τ, where a larger $c_{\rm max}$ leads to a longer τ, see also [60, 62]. Thanks to DQT, we can evaluate $\langle j(t)j\rangle_{\rm eq}^{(c)}$ on large clusters and obtain $C(t)$ in the thermodynamic limit for long times. While we here focus on $\beta = 0$, both DQT and NLCE allow for accurate calculations of $C(t)$ at $\beta > 0$ as well [56, 57, 60].

Unperturbed Dynamics. First, we study $C(t)$ in the unperturbed system $\mathcal{H}_0$, i.e., in the Heisenberg chain. (L now denotes the length of a single chain.) In Fig. 1 (a), $\langle j(t)j\rangle/L$ is shown for periodic boundary conditions (PBC), obtained by ED ($L = 18$) and DQT ($L = 32, 34, 36$) [56, 63]. While the curves for different L coincide at short times, the ED curve starts to deviate from the DQT data for $t \gtrsim 8$. Moreover, for $t \gtrsim 20$, $C(t)$ takes on an approximately constant value which decreases with increasing L [56]. Next, Fig. 1 (b) shows $C(t)$ for open boundary conditions (OBC), and additional system sizes $L = 38, 39$. Compared to the previous PBC data in Fig. 1 (a), the convergence towards the thermodynamic limit is considerably slower for OBC, and finite-size effects are more pronounced.

We now come to our NLCE results. In Fig. 1 (c), $C(t)$ is shown for various expansion orders $c_{\rm max} \leq 39$. For increasing $c_{\rm max}$, we find that $C(t)$ is converged up to longer

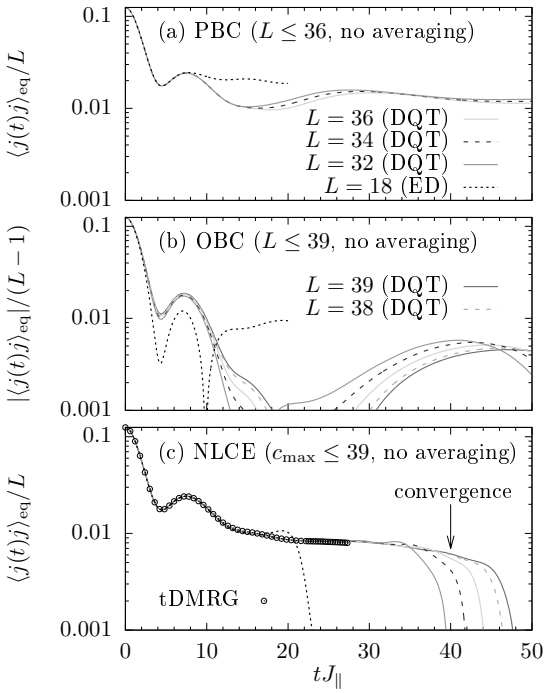

FIG. 1. (Color online) $C(t)$ for $J_\perp = 0$ at $\beta = 0$, obtained by ED ($L = 18$) and DQT ($L \leq 39$) for (a) PBC and (b) OBC. L here denotes the length of a single chain. (c): $C(t)$ obtained by NLCE up to expansion order $c_{\rm max} \leq 39$. As a comparison, we depict tDMRG data [38].

and longer times, until the expansion eventually breaks down. As a comparison, we also depict data obtained by the time-dependent density matrix renormalization group (tDRMG) [38, 64]. As becomes evident from Fig. 1 (c), tDMRG and NLCE agree perfectly for times $t \lesssim 27$. However, for the largest $c_{\rm max} = 39$ considered, the NLCE data actually is converged up to significantly larger times $t \approx 40$. This fact demonstrates that the combination of DQT and NLCE provides a powerful numerical approach to real-time correlation functions, and in comparison to Fig. 1 (a), also outperforms standard finite-size scaling on short to intermediate time scales. This determination of the unperturbed dynamics is important for this Letter and also extends earlier results presented in Ref. [60]. We have checked that NLCE data of similar quality can be obtained for other integrable models as well [32].

Perturbed Dynamics. Next, we come the actual discussion of $C(t)$ in spin ladders. While Fig. 2 (a) shows the second-order kernel $K_2(t) = {\rm Tr}\{i[j, \mathcal{V}_I(t)]i[j, \mathcal{V}]\}/{\rm Tr}\{j^2\}$, the respective decay rate $\gamma_2(t) = \int_0^t {\rm d}t' K_2(t')$ is shown in Fig. 2 (b) for various $L \leq 15$. On the one hand, for short times $t \lesssim 1$, we observe a linear growth $\gamma_2(t) \propto t$. On the other hand, for $t \gtrsim 2$, we find that $\gamma_2(t)$ first decreases slightly, but then starts to increase again. However, by comparing $\gamma_2(t)$ for different L, the latter apparently is a finite-size effect, and we expect the decay rate to be

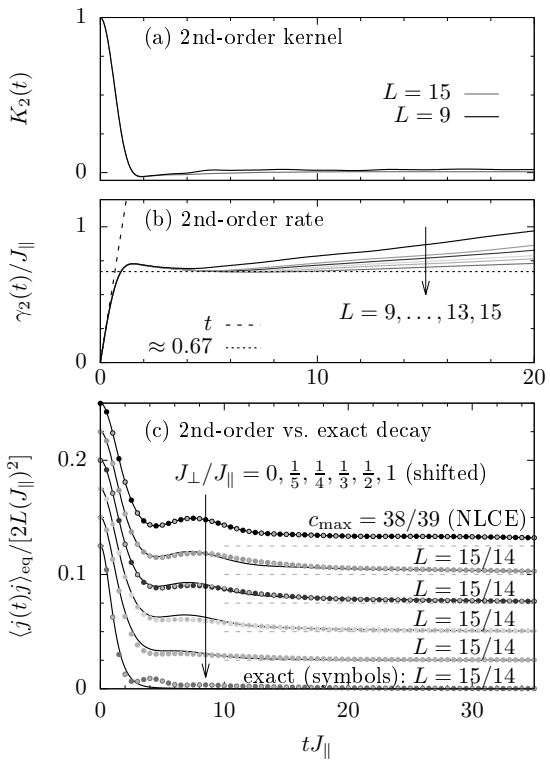

FIG. 2. (Color online) (a) and (b): Second-order kernel $K_2(t)$ and decay rate $\gamma_2(t)$ for various L. (c): $C(t)$ in spin ladders with several interchain couplings $J_\perp$ at $\beta = 0$, obtained by DQT for two different $L = 14, 15$ (small and large symbols). The curves indicate the prediction (8).

time-independent with $\gamma_2(t \gtrsim 8) \approx 0.67$ for $L \to \infty$.

In Fig. 2 (c), $C(t)$ is shown for several values of the interchain coupling $J_\perp/J_\parallel = 1/5, \ldots, 1$, i.e., for weak and also strong perturbations (vertically shifted for better visibility). We find that data for two different system sizes $L = 14, 15$ (symbols) perfectly coincide with each other, i.e., finite-size effect are negligible in the nonintegrable ladder. (For additional NLCE data, see [32].) Let us now compare this temporal decay of $C(t)$ to our prediction of an exponential damping. To this end, the unperturbed correlation function $C_0(t)$ as obtained by NLCE [Fig. 1 (c)] is exponentially damped according to

$$C(t) = C_0(t) \exp\left[-J_\perp^2 \int_0^t \mathrm{d}t' \gamma_2(t')\right] , \qquad (8)$$

where we have manually set $\gamma_2(t \geq 8) \equiv 0.67$ (see discussion above). Due to the linear growth of $\gamma_2(t)$ at short times, Eq. (8) leads to a Gaussian damping $\propto e^{-aJ_\perp^2 t^2}$ for $t \lesssim 1$, and turns into a conventional exponential damping $\propto e^{-bJ_\perp^2 t}$ for longer t. Remarkably, we find that Eq. (8) agrees very well with the exact $C(t)$ for all values of $J_\perp$ shown here, even though the perturbation is not weak. In particular, let us stress that there is no free parameter involved. This is a central result and confirms our theoretical arguments based on random matrices.

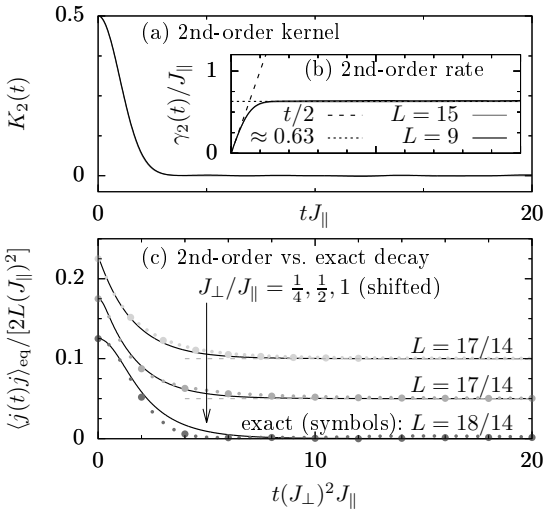

FIG. 3. (Color online) Analogous data as in Fig. 2, but now for the XX ladder.

In order to corroborate our findings further, let us study another but similar model. Namely, we consider the dynamics of $C(t)$ in the XX ladder, i.e., $\mathcal{H}_0$ and $\mathcal{V}$ are almost identical to Eq. (7), but the $S_l^z S_{l'}^z$-terms are absent. Note that, in this case, j is exactly conserved in the unperturbed system, $[\mathcal{H}_0, j] = 0$, and the decay of $C(t)$ is solely due to $\mathcal{V}$. Analogous to Fig. 2, the second-order kernel $K_2(t)$ and the decay rate $\gamma_2(t)$ are depicted in Figs. 3 (a) and (b), respectively. Comparing data for $L = 9, 15$, we observe that finite-size effects are negligible, and $\gamma_2(t) \approx 0.63$ becomes essentially constant for times $t \gtrsim 2$ [65]. Next, Fig. 3 (c) shows $C(t)$ for two different system sizes $L \leq 18$ (symbols), obtained by DQT for $J_\perp/J_\parallel = 1/4, 1/2, 1$ [66], as well as the the lowest-order prediction (8) (curves). (Recall that $C_0(t) = $ const. in this case.) Similar to Fig. 2 (c), we find that Eq. (8) describes the decay of $C(t)$ remarkably well, albeit the agreement is certainly better for smaller $J_\perp/J_\parallel$.

Conclusion. How does the expectation-value dynamics of some operator changes under a perturbation of the system's Hamiltonian? Based on projection operator techniques, we have answered this question for the case of a perturbation with random-matrix structure in the eigenbasis of the unperturbed Hamiltonian. As a main result, we have unveiled that such a (small) perturbation yields an exponential damping of the original reference dynamics, consistent with recent results in Ref. [21].

In addition, we have numerically confirmed that our findings are readily applicable to generic quantum many-body systems. In particular, we have illustrated that even a truncation to second order in the perturbation still provides a convincing description of the exact dynamics, also in cases where the perturbation is not weak.

Since an entirely random matrix structure of realistic physical perturbations might be questionable, promising directions of research include the identification of relevant substructures, as well as a better understanding of the pertinent correlations between matrix elements [32, 34].

Acknowledgments. This work has been funded by the Deutsche Forschungsgemeinschaft (DFG) - Grants No. 397107022 (GE 1657/3-1), No. 397067869 (STE 2243/3-1), No. 355031190 - within the DFG Research Unit FOR 2692. Additionally, we gratefully acknowledge the computing time, granted by the "JARA-HPC Vergabegremium" and provided on the "JARA-HPC Partition" part of the supercomputer "JUWELS" at Forschungszentrum Jülich.

* jonasrichter@uos.de
† jgemmer@uos.de
‡ rsteinig@uos.de

[1] U. Schollwöck, Ann. Phys. **326**, 96 (2011).
[2] I. Bloch, J. Dalibard, and W. Zwerger, Rev. Mod. Phys. **80**, 885 (2008).
[3] T. Langen, R. Geiger, and J. Schmiedmayer, Ann. Rev. Condens. Matter Phys. **6**, 201 (2015).
[4] A. Polkovnikov, K. Sengupta, A. Silva, and M. Vengalattore, Rev. Mod. Phys. **83**, 863 (2011).
[5] T. A. Brody, J. Flores, J. B. French, P. A. Mello, A. Pandey, and S. S. M. Wong, Rev. Mod. Phys. **53**, 385 (1981).
[6] O. Bohigas, M. J. Giannoni, and C. Schmit, Phys. Rev. Lett. **52**, 1 (1984).
[7] J. M. Deutsch, Phys. Rev. A **43**, 2046 (1991).
[8] M. Srednicki, Phys. Rev. E **50**, 888 (1994).
[9] M. Rigol, V. Dunjko, and M. Olshanii, Nature **452**, 854 (2008).
[10] C. W. von Keyserlingk, T. Rakovszky, F. Pollmann, and S. L. Sondhi, Phys. Rev. X **8**, 021013 (2018).
[11] A. Nahum, S. Vijay, and J. Haah, Phys. Rev. X **8**, 021014 (2018).
[12] V. Khemani, A. Vishwanath, and D. A. Huse, Phys. Rev. X **8**, 031057 (2018).
[13] J. Berges, Sz. Borsányi, and C. Wetterich, Phys. Rev. Lett. **93**, 142002 (2004).
[14] M. Moeckel and S. Kehrein, Phys. Rev. Lett. **100**, 175702 (2008).
[15] B. Bertini, F. H. L. Essler, S. Groha, and N. J. Robinson, Phys. Rev. Lett. **115**, 180601 (2015).
[16] T. Mori, T. N. Ikeda, E. Kaminishi, and M. Ueda, J. Phys. B **51**, 112001 (2018).
[17] P. Reimann and L. Dabelow, Phys. Rev. Lett. **122**, 080603 (2019).
[18] K. Mallayya, M. Rigol, and W. De Roeck, Phys. Rev. X **9**, 021027 (2019).
[19] M. Schmitt and S. Kehrein, Phys. Rev. B **98**, 180301(R) (2018).
[20] L. Knipschild and J. Gemmer, Phys. Rev. E **98**, 062103 (2018).
[21] L. Dabelow and P. Reimann, arXiv:1903.11881.
[22] A. Flesch, M. Cramer, I. P. McCulloch, U. Schollwöck, and J. Eisert, Phys. Rev. A **78**, 033608 (2008).
[23] S. Trotzky, Y-A. Chen, A. Flesch, I. P. McCulloch, U. Scholwöck, J. Eisert, and I. Bloch, Nat. Phys. **8**, 325 (2012).
[24] P. Barmettler, M. Punk, V. Gritsev, E. Demler, and E. Altman, Phys. Rev. Lett. **102**, 130603 (2009).
[25] K. Balzer, F. A. Wolf, I. P. McCulloch, P. Werner, and M. Eckstein, Phys. Rev. X **5**, 031039 (2015).
[26] S. Chaturvedi and F. Shibata, Z. Phys. B **35**, 297 (1979).
[27] H.-P. Breuer and F. Petruccione, *The Theory of Open Quantum Systems* (Oxford University Press, New York, 2007).
[28] Note that Eq. (1) strictly holds if there is no "inhomogeneity", i.e., we have to demand $\mathcal{P}_\omega\rho(0) = \rho(0)$. Even if this is not the case, the violation of (1) is expected to be minor for small λ [27].
[29] R. Steinigeweg and T. Prosen, Phys. Rev. E **87**, 050103(R) (2013).
[30] C. Bartsch, R. Steinigeweg, and J. Gemmer, Phys. Rev. E **77**, 011119 (2008).
[31] For time-dependent problems, a truncation to lowest order is in general (for nonrandom matrices) not meaningful a priori, even if the perturbation is small. For small perturbations, the relevant time scales are long and higher orders can become relevant on these time scales.
[32] See Supplemental Material for details on the matrix structure of the specific perturbation under consideration, as well as for additional NLCE data on the integrable Hubbard chain and the nonintegrable Heisenberg and XX ladders.
[33] J. Richter, J. Gemmer, and R. Steinigeweg, Phys. Rev. E **99**, 050104(R) (2019).
[34] L. Foini and J. Kurchan, Phys. Rev. E **99**, 042139 (2019).
[35] X. Zotos, Phys. Rev. Lett. **92**, 067202 (2004).
[36] P. Jung, R. W. Helmes, and A. Rosch, Phys. Rev. Lett. **96**, 067202 (2006).
[37] M. Žnidarič, Phys. Rev. B **88**, 205135 (2013).
[38] C. Karrasch, D. M. Kennes, and F. Heidrich-Meisner, Phys. Rev. B **91**, 115130 (2015).
[39] R. Steinigeweg, J. Herbrych, X. Zotos, and W. Brenig, Phys. Rev. Lett. **116**, 017202 (2016).
[40] Here, the current autocorrelation $C(t)$ can also be thought of as the expectation-value dynamics $\langle j(t)\rangle$, resulting from an initial state $\rho(0) \propto 1 + \varepsilon j$. Note that, in this case, there is no inhomogeneity [28, 41, 42].
[41] R. Steinigeweg and R. Schnalle, Phys. Rev. E **82**, 040103(R) (2010).
[42] R. Steinigeweg, Phys. Rev. E **84**, 011136 (2011).
[43] F. Heidrich-Meisner, A. Honecker, and W. Brenig, Eur. Phys. J. Spec. Top. **151**, 135 (2007).
[44] J. Sirker, R. G. Pereira, and I. Affleck, Phys. Rev. Lett. **103**, 216602 (2009).
[45] C. Karrasch, J. H. Bardarson, and J. E. Moore, Phys. Rev. Lett. **108**, 227206 (2012).
[46] J. Richter, F. Jin, L. Knipschild, J. Herbrych, H. De Raedt, K. Michielsen, J. Gemmer, and R. Steinigeweg, Phys. Rev. B **99**, 144422 (2019).
[47] J. Gemmer, M. Michel, and G. Mahler, *Quantum Thermodynamics* (Springer, Berlin, 2004).
[48] S. Popescu, A. J. Short, and A. Winter, Nat. Phys. **2**, 754 (2006).
[49] S. Goldstein, J. L. Lebowitz, R. Tumulka, and N. Zanghì, Phys. Rev. Lett. **96**, 050403 (2006).
[50] P. Reimann, Phys. Rev. Lett. **99**, 160404 (2007).

[51] C. Bartsch and J. Gemmer, Phys. Rev. Lett. **102**, 110403 (2009).
[52] A. Hams and H. De Raedt, Phys. Rev. E **62**, 4365 (2000).
[53] T. Iitaka and T. Ebisuzaki, Phys. Rev. Lett. **90**, 047203 (2003).
[54] S. Sugiura and A. Shimizu, Phys. Rev. Lett. **111**, 010401 (2013).
[55] T. A. Elsayed and B. V. Fine, Phys. Rev. Lett. **110**, 070404 (2013).
[56] R. Steinigeweg, J. Gemmer, and W. Brenig, Phys. Rev. Lett. **112**, 120601 (2014).
[57] R. Steinigeweg, J. Gemmer, and W. Brenig, Phys. Rev. B **91**, 104404 (2015).
[58] B. Tang, E. Khatami, and M. Rigol, Comput. Phys. Commun. **184**, 557 (2013).
[59] K. Mallayya and M. Rigol, Phys. Rev. Lett. **120**, 070603 (2018).
[60] J. Richter and R. Steinigeweg, Phys. Rev. B **99**, 094419 (2019).
[61] H. De Raedt and K. Michielsen, in *Handbook of Theoretical and Computational Nanotechnology* (American Scientific Publishers, Los Angeles, 2006).
[62] I. G. White, B. Sundar, and K. R. A. Hazzard, arXiv:1710.07696.
[63] J. Richter, F. Jin, H. De Raedt, K. Michielsen, J. Gemmer, and R. Steinigeweg, Phys. Rev. B **97**, 174430 (2018).
[64] D. M. Kennes and C. Karrasch, Comput. Phys. Commun. **200**, 37 (2016).
[65] In fact, since the XX chain can be brought into a quadratic form, $K_2(t)$ and $\gamma_2(t)$ could in principle even be obtained analytically for this particular case (see also [42]).
[66] R. Steinigeweg, F. Heidrich-Meisner, J. Gemmer, K. Michielsen, and H. De Raedt, Phys. Rev. B **90**, 094417 (2014).

SUPPLEMENTAL MATERIAL

MATRIX STRUCTURE OF THE PERTURBATION

Let us study if the realistic physical perturbation from the main part of this Letter is indeed compliant with a random-matrix description. Referring to Eq. (7), we have considered a spin-1/2 lattice model with ladder geometry, where the rung part of the ladder is treated as a perturbation, i.e., the Hamiltonian reads $\mathcal{H} = J_{\parallel}\mathcal{H}_0 + J_{\perp}\mathcal{V}$, with

$$\mathcal{H}_0 = \sum_{l=1}^{L}\sum_{k=1}^{2} \mathbf{S}_{l,k}\cdot\mathbf{S}_{l+1,k}\ ; \quad \mathcal{V} = \sum_{l=1}^{L} \mathbf{S}_{l,1}\cdot\mathbf{S}_{l,2}\ . \tag{S1}$$

In Fig. S1, the matrix representation of $\mathcal{V}$ in the eigenbasis of $\mathcal{H}_0$ is illustrated, where we restrict ourselves to a single symmetry subsector with magnetization $S^z = -1$, momentum $k = 2\pi/L$, and even parity $p = 1$. (Both $\mathcal{H}_0$ and $\mathcal{V}$ are entirely real in this case.) Moreover, we employ a suitable coarse graining according to [S1]

$$g(E,E') = \frac{\sum_{mn}|\mathcal{V}_{mn}|^2 D(\bar{E})}{D(E)D(E')}\,, \tag{S2}$$

where the sum runs over matrix elements $\mathcal{V}_{nm}$ in two energy shells of width $2\delta E$, $E_n \in [E-\delta E, E+\delta E]$ and $E_m \in [E'-\delta E, E'+\delta E]$. $D(E)$, $D(E')$, and $D(\bar{E})$ denote the number of states in these energy windows. This rough structure of $\mathcal{V}$ is shown in Figs. S1 (a) and (b), both for the Heisenberg ladder and the XX ladder. In both cases, we find that $\mathcal{V}$ exhibits a banded matrix structure with more spectral weight close to the diagonal. However, especially in the case of the XX ladder, $g(E,E')$ is not homogeneous within this band, but rather exhibits some fine structure.

For a more detailed analysis, a close-up of 200×200 matrix elements $\mathcal{V}_{mn}$ is shown in Figs. S1 (c) and (d). We find that there is a coexistence between regions where the $\mathcal{V}_{mn}$ appear to be random, and regions where the $\mathcal{V}_{mn}$ vanish (e.g. due to additional conservation laws). Moreover, in the case of the XX ladder, these regions are more extended.

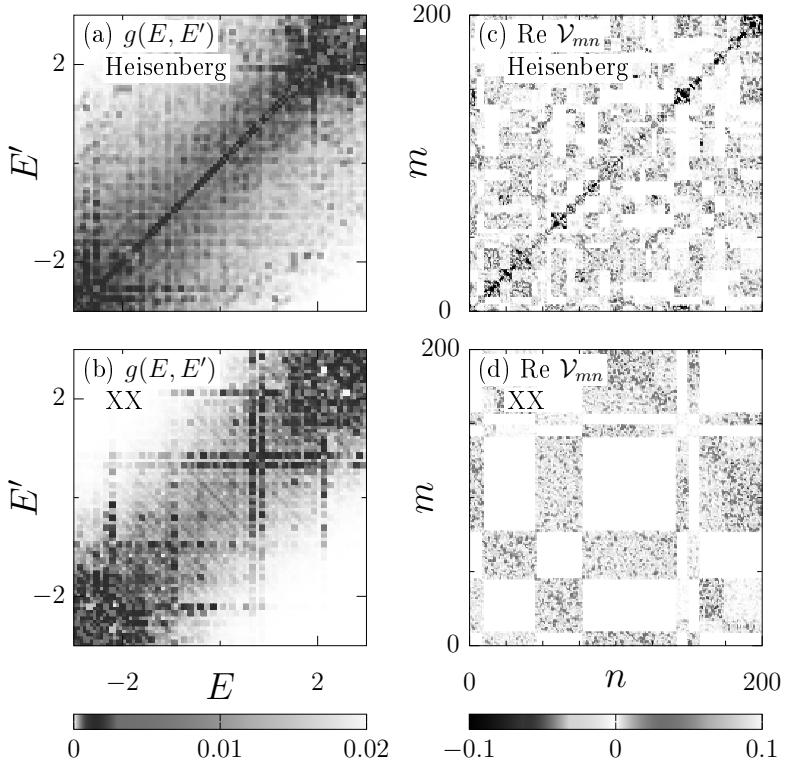

FIG. S1. (Color online) Matrix structure of $\mathcal{V}$ in the eigenbasis of $\mathcal{H}_0$ in the symmetry subsector with magnetization $S^z = -1$, momentum $k = 2\pi/L$, and even parity $p = 1$, both for the Heisenberg ladder (top) and the XX ladder (bottom). We have $L = 9$ in all cases.

Thus, the realistic $\mathcal{V}$ is certainly not an entirely random matrix. Nevertheless, as demonstrated in the main part, our theoretical arguments still apply remarkably well and $\mathcal{V}$ causes to good quality a damping of the unperturbed dynamics according to lowest-order perturbation theory. This can be understood due to the fact that bare randomness is not necessarily crucial for a successful truncation within the TCL approach. Rather, $\mathcal{V}$ is required to exhibit a so-called "Van Hove" structure [S2].

NLCE DATA FOR ANOTHER INTEGRABLE MODEL

In the main text, we have used a combination of DQT and NLCE to calculate the unperturbed dynamics of the spin-current autocorrelation in the integrable spin-1/2 Heisenberg chain. This combination has allowed us to obtain numerically exact information on rather long time scales, which cannot be reached in direct calculations in systems with periodic or open boundary conditions, due to significant finite-size effects. To illustrate that this combination of DQT and NLCE can yield also for other integrable models the reference dynamics with a similar quality, we show additional data for the Fermi-Hubbard chain, described by the Hamiltonian $\mathcal{H} = \sum_{l=1}^{L} h_l$,

$$h_l = -t_\mathrm{h} \sum_{s=\downarrow,\uparrow} (a_{l,s}^\dagger a_{l+1,s} + \mathrm{H.c.}) + U(n_{l,\downarrow} - \frac{1}{2})(n_{l,\uparrow} - \frac{1}{2}) \,, \tag{S3}$$

where the operator $a_{l,s}^\dagger$ ($a_{l,s}$) creates (annihilates) at site l a fermion with spin s, t_h is the hopping matrix element, and L is the number of sites. The operator $n_{l,s}$ is the local occupation number and U is the strength of the on-site interaction. For this model, we consider the particle current $j = \sum_{l=1}^{L} j_l$,

$$j_l = -t_\mathrm{h} \sum_{s=\downarrow,\uparrow} (i a_{l,s}^\dagger a_{l+1,s} + \mathrm{H.c.}) \,, \tag{S4}$$

and summarize our numerical results for the corresponding autocorrelation and $U = 4$ in Fig. S2. Apparently, the situation is like the one in Fig. 1 of the main text. On the one hand, in direct calculations with open or periodic boundary conditions, strong finite-size effects set in at short times, even for quite large L. On the other hand, NLCE for the largest expansion order c_max is converged to substantially longer times. Even though not shown explicitly, we have checked that a good convergence is also reached for $U = 8$. We thus expect that a perturbative analysis, as presented in this work, can be carried out for a wide class of quantum many-body systems, which we plan to do in detail in future work.

NLCE DATA FOR NONINTEGRABLE MODELS

While it is certainly possible to use NLCE also for nonintegrable models, finite-size effects in direct calculations are much less pronounced in these models, as evident from Figs. 2 and 3 of the main text. This is why we have not shown corresponding NLCE data in these figures and instead relied on pure DQT data for systems with periodic boundary conditions. To demonstrate that these DQT data are indeed in excellent agreement with NLCE data, we show in Fig. S3 corresponding numerical results for the Heisenberg and XX ladder, in both cases for $J_\perp/J_\parallel = 1$.

* jonasrichter@uos.de
† jgemmer@uos.de
‡ rsteinig@uos.de

[S1] J. Richter, J. Gemmer, and R. Steinigeweg, Phys. Rev. E **99**, 050104(R) (2019).
[S2] C. Bartsch, R. Steinigeweg, and J. Gemmer, Phys. Rev. E **77**, 011119 (2008).
[S3] C. Karrasch, D. M. Kennes, and J. E. Moore, Phys. Rev. B **90**, 155104 (2014).

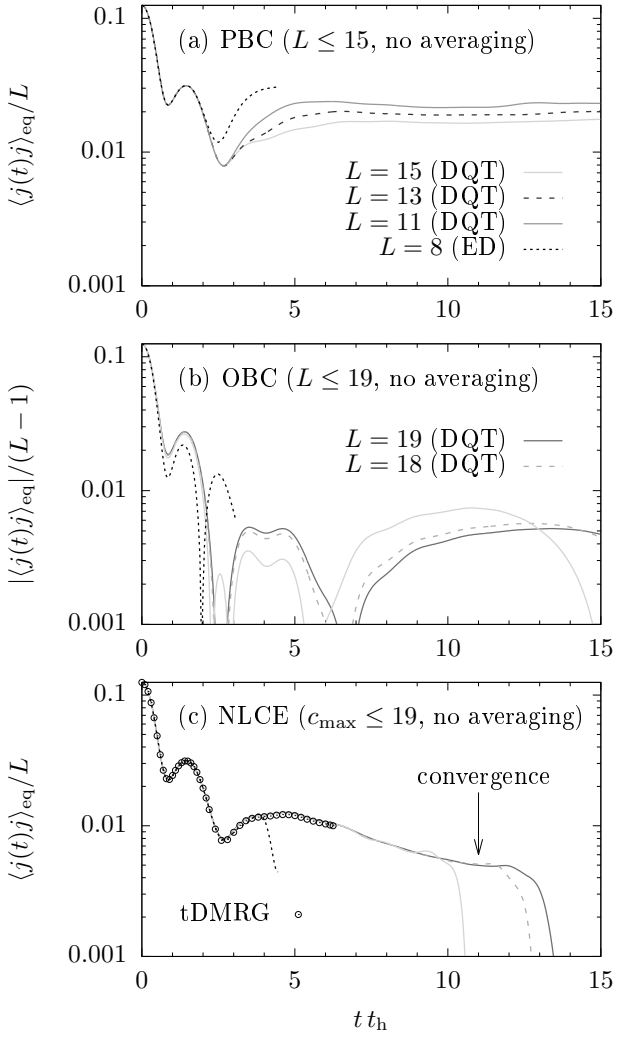

FIG. S2. (Color online) Current autocorrelation $C(t)$ in the Fermi-Hubbard chain ($U = 4$), obtained by ED ($L = 8$) and DQT ($L \leq 19$) at $\beta = 0$ for (a) periodic boundary conditions (PBC) and (b) open boundary conditions (OBC). (c) $C(t)$ obtained by NLCE up to expansion order $c_{\rm max} \leq 19$. As a comparison, we depict data from the time-dependent density matrix renormalization group (tDMRG) [S3].

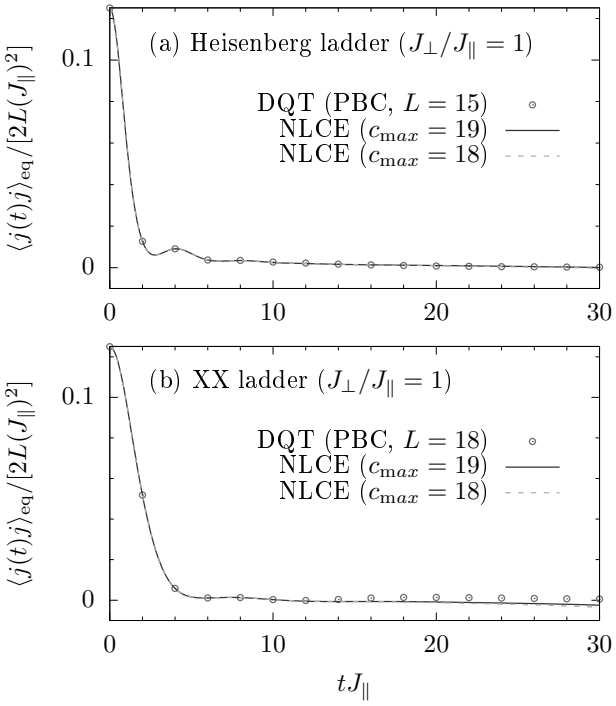

FIG. S3. (Color online) Current autocorrelation $C(t)$ for the (a) Heisenberg ladder and (b) XX ladder, in both cases for $J_\perp/J_\parallel = 1$. DQT data for periodic boundary conditions, as shown in the main text, is compared to NLCE data for two expansion orders $c_{\rm max} = 18$ and 19.